Operational Retrieval of Atmospheric Temperature, Moisture, and Ozone from MODIS Infrared Radiances

Jun Li[@], Suzanne Wetzel Seemann[@], W. Paul Menzel[*], Liam E. Gumley[@]

[@] Cooperative Institute for Meteorological Satellite Studies, University of Wisconsin-Madison

[*] Office of Research and Applications, NOAA/NESDIS

Manuscript prepared for submission to *Journal of Applied Meteorology*: June 12, 2002

Corresponding author's address:

Suzanne Wetzel Seemann
CIMSS/SSEC
University of Wisconsin-Madison
1225 West Dayton St.
Madison, WI 53706

E-mail: swetzel@ssec.wisc.edu
Tel: (608) 265-5357
Fax: (608) 262-5974

Abstract

The algorithm for operational retrieval of atmospheric temperature and moisture profiles, total column ozone, and surface skin temperature from the Moderate-Resolution Imaging Spectroradiometer (MODIS) longwave infrared radiances is presented. The retrieval algorithm, MOD07_L2, uses clear-sky radiances measured by MODIS over land and ocean for both day and night in a statistical retrieval with an option for a subsequent nonlinear physical retrieval. The regression coefficients for the statistical retrieval are derived using a fast radiative transfer model with input taken from a data set of global radiosondes of atmospheric temperature, moisture and ozone profiles. Validation of atmospheric temperature and moisture profiles and total precipitable water vapor (TPW) is performed by a comparison with data from ground-based instrumentation at the Atmospheric Radiation Measurement-Cloud and Radiation Testbed (ARM-CART) in Oklahoma. Comparisons over one year show the operational regression-based MODIS TPW agrees with the microwave radiometer (MWR) TPW at the ARM-CART site in Oklahoma with an RMS of 3.6 mm. For moist cases with TPW greater than 17 mm, the physical retrieval improves the RMS to less than 3 mm. For dry atmospheres (TPW less than 10mm), both physical and regression-based retrievals from MODIS radiances tend to overestimate the moisture. Global maps of MODIS atmospheric products are compared with the Special Sensor Microwave/Imager (SSM/I) moisture and Total Ozone Mapping Spectrometer (TOMS) ozone products. MODIS temperature, moisture, and ozone products are in general agreement with the gradients and distributions from the other satellites, while MODIS depicts more detailed structure with its improved spatial resolution.

1. Introduction

The development of global climate and weather models requires accurate monitoring of atmospheric temperature and moisture as well as trace gases and aerosols. Until recently, continuous monitoring of changes in these parameters on a global scale has been difficult. The Moderate Resolution Imaging Spectroradiometer (MODIS) instrument, launched on December 18, 1999 onboard the National Aeronautics and Space Administration (NASA)'s Earth Observing System (EOS) Terra platform, offers a new opportunity to improve global monitoring of temperature, moisture, and ozone distributions and changes therein. MODIS is a scanning spectroradiometer with 36 visible (VIS), near infrared (NIR), and infrared (IR) spectral bands between 0.645 and 14.235 μm (King et al. 1992). Table 1 summarizes the MODIS technical specifications and Table 2 lists the MODIS spectral bands. Figure 1 shows the spectral responses of the MODIS infrared bands in relation to an atmospheric emission spectrum computed by a line-by-line radiative transfer model (LBL-RTM) for the U.S. standard atmosphere.

The wide spectral range, high spatial resolution and near-daily global coverage enable MODIS to observe the Earth's atmosphere and continuously monitor changes. MODIS retrievals of atmospheric water vapor and temperature are intended to advance a better understanding of the role played by energy and water cycle processes in determining the Earth's weather and climate. MODIS temperature and moisture products can be used together with other satellite measurements in numerical weather prediction models in the regions where conventional meteorological observations are sparse. Determination and validation of various land, ocean, and atmospheric products such as sea surface temperature, land surface temperature,

and ocean aerosol properties require temperature and moisture profiles as well as total ozone at MODIS spatial resolution as ancillary input.

The advantage of MODIS for retrieving atmospheric profiles is its combination of shortwave and longwave infrared spectral bands (3 – 14.5μm) useful for sounding and its high spatial resolution suitable for imaging (1km at nadir). The increased spatial resolution of MODIS measurements delineates horizontal gradients of moisture, temperature, and atmospheric total ozone better than companion instruments such as the Geostationary Operational Environmental Satellite (GOES) sounder (10 km resolution for single field of view retrievals), Advanced Microwave Sounding Unit-A (AMSU-A, 45 km resolution), High-resolution Infrared Radiation Sounder (HIRS, 19km resolution), and the Atmospheric Infrared Sounder (AIRS, 15km resolution). However, as MODIS has broadband spectral resolution, there is only modest information content regarding vertical profiles. Sounder radiances with higher spectral resolution such as AIRS and CrIS (Cross-Track Interferometer Sounder) of the National Polar Orbiting Environmental Satellite System (NPOESS) (http://www.npoess.noaa.gov) contain more information about the atmospheric vertical distribution of temperature and moisture.

This paper details the operational MODIS MOD07_L2 algorithm for retrieving vertical profiles of atmospheric temperature and moisture, total column ozone burden, and integrated precipitable water vapor. The retrievals are performed using clear sky radiances measured by MODIS within a 5x5 field of view (approximately 5km resolution) over land and ocean for both day and night. A version of the algorithm is operational at the Goddard Distributed Active Archive Center (GDAAC) processing system (http://daac.gsfc.nasa.gov/MODIS). Section 2 describes the retrieval algorithm. Section 3 outlines the implementation of the retrieval, including cloud detection, radiance bias adjustments, the training data set, and a technique for

eliminating the IR shortwave surface emissivity uncertainty in the retrievals. Section 4 presents some validation of MODIS atmospheric products. A discussion of retrieval errors and other issues affecting the atmospheric retrieval is in section 5. Section 8 offers some conclusions and plans for future work.

2. Algorithm Development

The MODIS atmospheric profile algorithm is a statistical regression with the option for a subsequent non-linear physical retrieval. The retrieval procedure involves linearization of the radiative transfer model and inversion of radiance measurements. To derive the statistical regression coefficients, MODIS infrared band radiances are calculated from radiosonde observations of the atmospheric state, generating calculated radiance/observed atmospheric profile pairs. The radiative transfer calculation of the MODIS spectral band radiances is performed using a transmittance model called Pressure layer Fast Algorithm for Atmospheric Transmittances (PFAAST) (Hannon et al. 1996, Eyre and Woolf 1988); this model has 101 pressure level vertical coordinates from 0.05 to 1100 hPa. The calculations take into account the satellite zenith angle, absorption by well-mixed gases (including nitrogen, oxygen, and carbon dioxide), water vapor (including the water vapor continuum), and ozone. The retrieval algorithms are developed in this section.

2.1 Radiative transfer model and its linearization

If scattering by the atmosphere is neglected, the true clear radiance exiting the earth-atmosphere system for a given MODIS IR band with center wavenumber n is approximated by

$$R_n = eB_s t_s - \int_0^{p_s} B dt(0,p) + (1-e)\int_0^{p_s} B dt^* + R^{'}, \qquad (1)$$

R_n is the spectral radiance, $t(0, p)$ is the total transmittance from top of the atmosphere to the atmospheric pressure p, e is the surface emissivity, B is the Planck radiance which is a function of pressure p, subscript s denotes surface, $t^* = t_s^2 / t$ is the downwelling transmittance, and $R^{'}$ represents the contribution of reflected solar radiation in the infrared region. The reflected infrared solar radiation can be eliminated for bands with wavelengths longer than 4.0 m m during the day.

If the MODIS observed radiance R_n^m of each band is known, then R_n^m can be considered a non-linear function of the atmospheric properties, including the temperature profile, water vapor mixing ratio profile, ozone mixing ratio profile, surface skin temperature, and surface emissivity. That is $R_n^m = R_n(T, q, O_3, T_s, e, ...) + s_n$ (s_n is the instrument noise and other source of error), or in general

$$Y^m = Y(X) + s \ , \qquad (2)$$

where the vector X contains L (levels of atmosphere) atmospheric temperatures, L atmospheric water vapor mixing ratios, L atmospheric ozone mixing ratios (the water vapor or ozone is expressed as the logarithm of the mixing ratio in practical applications), one surface skin temperature, 2 infrared surface emissivities at 909 and 2500 wavenumbers, and Y^m contains N (number of MODIS spectral bands used) observed radiances.

To linearize Eq.(1) the first order variations $dB = \frac{\partial B}{\partial T} dT$ and $dR = \frac{\partial R}{\partial Tb} dTb$ are used, define $b(p) = \frac{\partial B / \partial T}{\partial R / \partial Tb}$. The linearized form of Eq.(1) is:

$$dTb_n = W_{T_s} dT_s + \int_0^{p_s} W_T dT dp + \int_0^{p_s} W_q d \ln q dp + \int_0^{p_s} W_{o_3} d \ln o_3 dp \,, \qquad (3)$$

where W_T, W_q and W_{o_3} are the weighting functions (sensitivity functions) of the atmospheric temperature profile, water vapor mixing ratio profile, and ozone mixing ratio profile, respectively. The weighting functions can be calculated efficiently from a given atmospheric state (Li 1994, Li et al. 2000):

$$W_{T_s} = b_s t_s e , \tag{4a}$$

$$W_T(p) = -b\frac{\partial t}{\partial p} + b(1-e)\frac{\partial t^*}{\partial p} , \tag{4b}$$

$$\begin{aligned} W_q(p) = &\{(T_s - T_a)e t_s b_s - 2(1-e)\int_0^{p_s} b\, t^* \frac{\partial T}{\partial p} dp\}\frac{\partial \ln t_q}{\partial p} \\ &+ \{\int_p^{p_s} b[[t + (1-e)t^*]\frac{\partial T}{\partial p} dp\}\frac{\partial \ln t_q}{\partial p} \end{aligned} , \tag{4c}$$

$$\begin{aligned} W_{o_3}(p) = &\{(T_s - T_a)e t_s b_s - 2(1-e)\int_0^{p_s} b\, t^* \frac{\partial T}{\partial p} dp\}\frac{\partial \ln t_{o_3}}{\partial p} \\ &+ \{\int_p^{p_s} b[[t + (1-e)t^*]\frac{\partial T}{\partial p} dp\}\frac{\partial \ln t_{o_3}}{\partial p} \end{aligned} , \tag{4d}$$

Tb_n is the brightness temperature for the MODIS IR spectral band with center wavenumber n. t_q and t_{o_3} are the water vapor and ozone component transmittance functions, respectively.

Figure 2 shows the temperature weighting functions for the MODIS IR bands 20-25 and bands 27-36 calculated from a U.S. standard atmosphere. Bands 27 and 28 are water vapor absorption bands; they also provide information about the atmospheric temperature if there is enough moisture in the atmosphere. Bands 33–36 are CO_2 absorption bands that provide atmospheric temperature information; they can be used to infer the cloud properties with a known atmospheric temperature profile (Frey et al. 1999; Li et al. 2001). The moisture weighting functions in Figure 3 show that bands 27 and 28 provide information about the distribution of

moisture in the troposphere, and that the window bands also provide some moisture information due to weak water vapor absorption. The weighting functions shown in Figures 2 and 3 were computed without any contrast between surface air temperature and surface skin temperature. The weighting functions show MODIS has limited skill in retrieving boundary layer temperature and moisture information. However, if a large (e.g., greater than 5 ^{o}K) contrast exists between the surface air temperature and surface skin temperature, information about the boundary layer moisture structure can be retrieved with some success (see Figure 4). Increased sensitivity to moisture can be seen in Figure 4 near the surface, particularly in the window channels (bands 29, 31, and 32).

2.2 Regression retrieval processing

A computationally efficient method for determining temperature and moisture profiles from satellite sounding measurements uses previously determined statistical relationships between observed or modeled radiances and the corresponding atmospheric profiles. This method is often used to generate a first-guess for a physical retrieval algorithm, as is done in the International TOVS Processing Package (ITPP, Smith et al., 1993). The statistical regression algorithm for atmospheric temperature is described in detail in Smith et. al. (1970), and is summarized below for cloud-free skies.

The general inverse solution of Eq. 2 for the atmospheric profile can be written as (Smith 1970)

$$X = AY \; . \qquad (5)$$

The statistical regression algorithm seeks a "best-fit" operator matrix A that is computed using least squares methods with a large sample of atmospheric temperature and moisture soundings, and collocated radiance observations. Minimizing the error

$$\frac{\partial}{\partial A}\left|AY - X\right|^2 = 0, \tag{6}$$

yields

$$A = \left(Y^T Y\right)^{-1} Y^T X, \tag{7}$$

where $\left(Y^T Y\right)$ is the covariance of the radiance observations, and $\left(Y^T X\right)$ is the covariance of the radiance observations with the atmospheric profile.

Ideally, the radiance observations Y would be taken from actual MODIS measurements and used with time and space collocated radiosonde profiles X to directly derive the regression coefficients A. In such an approach, the regression relationship would not involve any radiative transfer calculations. However, radiosondes are routinely launched only two times each day at 0000 UTC and 1200 UTC simultaneously around the earth; Terra passes occur at roughly 1100-1200 AM and 1000-1100 PM local standard time each day. It is therefore not possible to obtain many time and space collocated MODIS radiances. Alternatively, the regression coefficients can also be generated from MODIS radiances calculated using a transmittance model with profile input from a global temperature and moisture radiosonde database. In this approach, the accuracy of the atmospheric transmittance functions for the various spectral bands is crucial for accurate parameter retrieval.

In the regression procedure, the primary predictors (Y in Eq.5) are MODIS infrared spectral band brightness temperatures. The algorithm uses 12 infrared bands with wavelengths between 4.465 μm and 14.235 μm. Surface emissivity effects in the short wave window bands are

mitigated by regressing against band differences (e.g., instead of BT(4.5 μm) and BT(4.4 μm) we use the difference, BT(4.5 μm) - BT(4.4 μm) in the regression, where BT represents brightness temperature). Estimates of surface pressure are also used as predictors to improve the retrieval. Table 3 lists the predictors and their noise used in the regression procedure. Quadratic terms of all brightness temperatures in Table 3 are also used as predictors to account for the non-linear relationship of moisture to the MODIS radiances. The noise used in the algorithm is larger than estimates of post-launch detector noise in order to account for variability between the ten detectors (striping). The regression coefficients are generated for 680 local zenith angles from nadir to 65^{o}, and various IR emissivity spectra are assigned to the training profiles to account for varying surface properties in the regression procedure.

In the MODIS retrieval algorithm, a global data set of radiosonde observations (the NOAA-88b data set) is used in the calculations. The original NOAA-88b data contains 7547 globally distributed clear sky radiosonde profiles of temperature, moisture, and ozone, along with observations of surface temperature and pressure. Additional radiosondes have been added to this data set in the MODIS algorithm, as described in section 3.3. The radiative transfer calculation of the MODIS spectral band radiances is performed with the PFAAST model for each profile from the training data set to produce a temperature-moisture-ozone profile/MODIS radiance pair. The estimated MODIS instrument noise is added to the calculated spectral band radiances. The regression coefficients (see Eq.(7)) are then generated using these calculated radiances and the matching atmospheric profile. To perform the regression, Eq.(5) can be applied to the actual MODIS measurements to obtain the estimated atmospheric profiles; integration yields the total precipitable water or total column ozone. The advantage of this approach is that it does not need MODIS radiances collocated in time and space with

atmospheric profile data; it requires only historical profile observations. However, it involves the radiative transfer calculations and requires an accurate forward model in order to obtain a reliable regression relationship. Any uncertainties (e.g., a bias of the forward model) in the radiative calculations will influence the retrieval. To address model uncertainties, radiance bias adjustments have been implemented in the retrieval algorithm, as discussed in section 3.2.

2.3 Non-linear physical retrieval processing

The statistical regression algorithm has the advantage of computational efficiency, numerical stability, and simplicity. However, it does not account for the physical properties of the radiative transfer equation (RTE). After computing atmospheric profiles from the regression technique, a non-linear iterative physical algorithm (Li et al., 2000) applied to the RTE often improves the solution. The physical retrieval approach is described in this section.

The physical procedure is based on the regularization method (Li et al., 2000) wherein a penalty function defined by

$$Y(X) = \left\| Y^m - Y(X) \right\|^2 + g \left\| X - X_0 \right\|^2 \qquad (8)$$

is minimized to improve the fit of the MODIS spectral band measurements to the regression first guess. In equation 8, X is the atmospheric profile to be retrieved, X_0 is the initial state of the atmospheric profile or the first guess from regression, Y^m is the vector of the observed MODIS brightness temperatures used in the retrieval process, $Y(X)$ is the vector of calculated MODIS brightness temperatures from an atmospheric state (X), and g is the regularization parameter that can be determined by the Discrepancy Principle (Li and Haung, 1999; Li et al. 2000). The solution provides a balance between MODIS spectral band radiances and the first guess. If a radiative transfer calculation using the first guess profile as input fits all the MODIS spectral

band radiances well, less weight is given to the MODIS measurements in the non-linear iteration, and the solution will be only a slight modification of the first guess. However, if the first guess does not agree well with the MODIS spectral band radiances, then the iterative physically retrieved profile will be given a larger weight. Thus, the temperature, moisture, and ozone profiles as well as the surface skin temperature will be modified in order to obtain the best simultaneous fit to all the MODIS spectral bands used. For more details, see Li et al. (2000).

A comparison between the regression-based first guess brightness temperatures and the physical retrieval brightness temperatures is presented in Figure 5. The root-mean-squared (RMS) of observed minus retrieved brightness temperature decreases from the regression-based guess to the physical retrieval. The most significant improvement is apparent in the window bands 31 and 32, with the RMS decreasing from 1.0 ^{o}K to 0.57 ^{o}K (band 31, 11μm) and 1.28 ^{o}K to 0.78 ^{o}K (band 32, 12μm). When the RMS is computed for only moist cases with TPW greater than 17 mm, the physical retrieval errors are reduced even further to 0.1 ^{o}K for band 31 and 0.18 ^{o}K for band 32.

The improvements evident in the radiance calculations using the physical algorithm are also apparent in the retrieved products. For 20 clear-sky cases between April 1, 2001 and April 1, 2002 with a relatively moist atmosphere (TPW greater than 17mm), TPW computed by the physical retrieval and the regression retrieval were compared with that measured by the Southern Great Plains (SGP) Atmospheric Radiation Measurement-Cloud and Radiation Testbed (ARM-CART) microwave radiometer (MWR). On average over these cases there was improvement from the physical over the statistical retrieval; the RMS of MWR minus MODIS decreased by 0.9 mm, to 2.9 mm for the physical retrieval. Only moist cases were used in this comparison

because the current physical retrieval algorithm has very little effect on dry cases; the moisture signal is weak in the MODIS IR radiance measurements for a dry atmosphere.

In summary, a non-linear physical retrieval shows some improvement over a regression retrieval for MODIS retrievals. However, the physical retrieval requires more computation time and, like the regression used in the MODIS processing, is dependent on the accuracy of the radiative transfer model.

3. Operational Implementation

The operational MODIS retrieval algorithm consists of several procedures that include cloud detection, averaging clear radiances from 5 by 5 field-of-view (FOV) areas, bias adjustment of MODIS brightness temperatures to account for forward model and instrument errors, regression retrieval, and an option to perform a physical retrieval. Because of computer limitations, the MODIS MOD07_L2 retrieval algorithm that is operational at GDAAC processing system includes only the regression retrieval. A version of the algorithm with the physical retrieval will be available for MODIS direct broadcast processing as part of the International MODIS/AIRS Processing Package (IMAPP) developed at the Space Science and Engineering Center (SSEC) at the University of Wisconsin-Madison (http://cimss.ssec.wisc.edu/~gumley/IMAPP/IMAPP.html).

3.1 Cloud detection algorithm

MODIS atmospheric and surface parameter retrievals require clear sky measurements. The operational MODIS cloud mask algorithm (Ackerman et al. 1998) is used to identify pixels that are cloud free. The MODIS cloud mask algorithm determines if a given pixel is clear by

combining the results of several spectral threshold tests. A confidence level of clear sky for each pixel is estimated based on a comparison between observed radiances and specified thresholds. The operational retrieval algorithm requires at least 5 of the 25 pixels in a 5x5 field-of-view area to have been assigned a 95% or greater confidence of clear by the cloud mask. The retrieval for each 5x5 field-of-view area is performed using the average radiance of those pixels that were considered clear. Since the decision to perform a retrieval depends on the validity of the cloud mask algorithm, cloud contamination may occur if the cloud mask fails to detect a cloud, or the retrieval may not be run if the cloud mask falsely identifies a cloud.

3.2 Radiance bias adjustment in the retrieval processing

The forward model-calculated radiances have biases with respect to the MODIS measured radiances. There are several possible causes including calibration errors, spectral response uncertainty, temperature and moisture profile inaccuracies, and forward model error. The statistical regression and the physical retrieval methods use both measured and calculated radiances and thus require that this bias be minimized. Techniques developed for computing GOES sounder radiance biases with respect to the forward model (Hayden 1988) were employed in the MODIS atmospheric profile algorithm. Bias adjustment for radiative transfer calculation of MODIS spectral band radiances is demonstrated to have a positive impact on the atmospheric product retrievals.

Radiance bias calculations are routinely computed for the SGP ARM-CART site for clear scenes with MODIS sensor zenith angle less than 35^{o}. Observed MODIS radiances, averaged from a 5x5 field-of-view area, were compared with those computed by the same transmittance model used in the algorithm. The calculations of radiances were performed using the 101-level

PFAAST model, with temperature and moisture profile input from National Center for Environmental Prediction's Global Data Analysis System (NCEP-GDAS) global analysis data. Skin temperature and emissivity estimates came from regression with MODIS radiances. To establish credibility for the regression-derived skin temperature input, actual observed skin temperature from a ground-based downward-looking infrared thermometer (IRT) that measures the radiating temperature of the ground surface (http://www.arm.gov/docs/instruments/static/irt.html) was also used. Figure 6 shows that, on average over 63 clear-sky day and night cases from April 2001 to June 2002, the biases computed using the regression-based skin temperature differ very little from those computed using the IRT skin temperature. A comparison of the two skin temperatures for the same cases (Figure 7) shows reasonable agreement; the RMS of the IRT skin temperature minus MODIS regression-based skin temperature is 1.7 ^{o}K, and the slope of a linear best-fit line is 1.01.

Most CART site MODIS radiance biases (observed minus calculated BT) shown in Figure 6 are positive, indicating that, on average, the observed MODIS brightness temperatures are warmer than those predicted by the model. Case-to-case variability for each spectral band can be seen in Figure 8; the high variability in the biases for band 27 is a result of the significant detector-to-detector noise, or striping, that exists in the radiance data for this band.

A comparison of MODIS products at the SGP ARM-CART site with and without the bias correction (not shown) confirms a significant improvement with the bias corrections. The RMS for the CART site MWR minus MODIS decreased from 4.9 mm to 3.6 mm when the bias corrections were applied. The improvements were primarily apparent for moist cases where the bias correction helped to correct a dry bias. Because the MODIS retrieval algorithm is applied globally, the biases computed at the SGP ARM-CART site are not appropriate for application at

other latitudes and for other ecosystem types. Thus, biases have been computed for other regions of the globe; however, they are less well validated. Future versions of the algorithm will include a more advanced global bias scheme that uses a regression based on air-mass predictors (atmospheric layer thickness, surface skin temperature, and TPW) such as that employed on the TIROS Operational Vertical Sounder (TOVS) (Eyre 1992; Harris and Kelly, 2001).

To compute the global radiance biases, observed MODIS brightness temperatures were compared with calculated brightness temperatures for 270 clear-sky scenes from June 2 - 5, 2001 with MODIS viewing zenith angle < 30^o. Calculations of brightness temperatures were performed as outlined above with skin temperature estimated from regression of MODIS radiances. As there are known difficulties in retrieving skin temperature and emissivity over the desert, these cases were excluded from the global averages. The global biases are separated into twelve groups: six latitude zones: north tropical (latitude 0^o to $+30^o$), south tropical (0^o to -30^o), north mid-latitude ($+30^o$ to $+50^o$), south mid-latitude (-30^o to -50^o), north polar (50^o to 90^o), south polar (-50^o to -90^o), each for land and ocean. The average global biases for north mid-latitude land agree fairly well with the CART site biases; the RMS of the MODIS-MWR TPW for 63 cases increased only 0.2 mm when using the global north mid-latitude biases instead of the CART site biases.

The radiance bias corrections applied in the operational MODIS atmospheric retrieval algorithm will be updated regularly to account for adjustments in the instrument calibration and improvements in the forward model. In addition, the bias values may vary seasonally so the bias corrections calculated from four days in June may need to be updated. Averaging of 63 CART site biases over a year by month (Figure 9) indicates that in northern Oklahoma, there may be a systematic annual variation in some bands. The water vapor band 27, for example, appears to

have larger observed-calculated biases in late fall and winter. More cases are needed to accurately determine the seasonal variability of the bias corrections.

3.3 Adjustments to the NOAA-88b training data set

The NOAA-88b data set contains 7547 globally distributed clear sky radiosonde observations and surface data from 1988. Profiles of temperature, moisture, and ozone and surface data from this data set were used to compute the regression coefficients for the MODIS statistical retrieval. To limit the retrievals to training data with physical relevance to the observed conditions, the NOAA-88b data was partitioned into seven zones based on the 11μm brightness temperatures (BT11) calculated from the profiles. The seven zones are BT11 < 245, 245-269, 269-285, 285-294, 294-300, 300-310, and > 310^{o}K. When each statistical retrieval is performed, it uses only the subset of the training data corresponding to BT11.

After partitioning, there was insufficient training data in the NOAA-88b data set for the very warm surfaces (the last two zones, BT11 > 300 ^{o}K). Figure 10 shows that many measurements over the north African deserts had BT11 > 300^{o}K. To address this problem, new radiosonde data from the north African desert regions for January – December 2001 were added to the training data set. 900 new radiosondes, spread equally through the twelve months, met the criteria of relative humidity < 90% at each level and physically reasonable behavior up to 100hPa; profiles of temperature and moisture from these radiosondes were added to the NOAA-88b data set. Figure 11 compares the 11μm brightness temperatures computed from the original NOAA-88b data set with those from the enhanced data set including the extra desert profiles.

Partitioning the BT11 into seven zones and adding training data improves the MODIS TPW retrievals; one example of such a case is presented here. Radiance and true color

reflectance images from 20 August 2001 are shown in Figure 12. A large area of clear sky exists from Texas through Oklahoma and southeastern Kansas. Figure 13 compares GOES-8 TPW with MODIS TPW from the old and new regressions; the new MODIS results compare better with the GOES than the old. The area in Kansas and Oklahoma that shows the most improvement has a warm BT11 that falls within the highest two classes (see Figure 14). This is consistent with results of other cases; the most significant improvements occurred for scenes with BT11 in the two highest classes.

3.4 Surface emissivity for IR 4.5mm spectral bands

The infrared surface emissivity in the NOAA-88b training data is variable for different atmospheric profiles, with a mean of 0.95 for longwave IR bands (9 – 13 μm bands) and 0.85 for shortwave IR bands; the standard deviation is 0.05 for both longwave and shortwave. In most situations the training data set accounts for the global emissivity variations. However, for some regions such as the deserts of north Africa, the surface emissivity has the potential to be significantly lower at 4 μm than at 11 μm (Salisbury and D'Aria 1992). Figure 15 shows emissivity spectral measurements from data obtained through the NASA Jet Propulsion Lab's spectral library (http://speclib.jpl.nasa.gov) for two silicates commonly found in desert regions, cyclosilicates and tectosilicates. The emissivity at the 4.5 μm spectral region is extremely low for both minerals, indicating that emissivities in the desert may be as low as 30-40%. Because emissivities this low are not included in the training data set, the IR 4.4 μm and 4.5 μm (bands 24 and 25) were not accurately represented and the MODIS retrievals were excessively moist in the desert regions. To remedy this problem, the difference between these two bands is used as a single predictor instead of using bands 24 and 25 independently; this subtraction removes most

of the surface emissivity signal in the regression equation. Brightness temperature increments for band 24, band 25, and the difference band 25 – band 24 with respect to emissivity are shown in Figure 16. The BT difference between band 25 and band 24 is found to be much less sensitive to the surface emissivity change than the BT of either band 24 or band 25 independently.

4. Validation of MOD07 products

Atmospheric retrievals from MODIS and other observing systems have been compared at three spatial scales: a) a fixed point with ground-based measurements (SGP ARM-CART), b) the continental scale with GOES sounder products, and c) the global scale with retrievals from the Special Sensor Microwave/Imager (SSM/I) and Total Ozone Mapping Spectrometer (TOMS).

4.1 Comparison of MODIS temperature and moisture with ARM-CART observations

Specialized instrumentation at the Southern Great Plains (SGP) Atmospheric Radiation Measurement-Cloud and Radiation Testbed (ARM-CART) in Oklahoma facilitates comparisons of MODIS atmospheric products with other observations collocated in time and space. Terra passes over the SGP CART daily between 0415-0515 UTC and 1700-1800 UTC. Radiosondes are launched three times each day at approximately 0530, 1730, and 2330 UTC. Observations of total column moisture are made by the microwave radiometer (MWR) every 40-60 seconds. An additional comparison is possible with the GOES-8 sounder (Menzel and Purdom 1994; Menzel et al. 1998) that retrieves TPW hourly.

MODIS retrieved products were compared for 64 clear-sky cases from April 2001 to June 2002. Manual inspection of visible and infrared images excluded any scenes with the possibility

of cloud contamination. MODIS sensor zenith angle was less than 50^{o} to the CART site for all cases.

TPW from MODIS regression retrievals, the GOES-8 sounder, radiosondes, and the MWR are compared in Figure 17. MODIS shows general agreement with the MWR for these cases; GOES-8 sounder and radiosondes show better agreement with the MWR. The RMS difference between MODIS and MWR TPW collocated in time and space is 3.6 mm for regression retrievals, compared with 1.78 mm and 1.16 mm for GOES-8 and radiosondes, respectively. For dry atmospheres, MODIS consistently overestimates the total column moisture; the average TPW bias (MODIS minus MWR) is approximately 3 mm for the 26 dry cases with MWR TPW less than 10 mm. Stephens et al. (1994) observed similar behavior in TOVS total column water vapor and attributed it to a limitation of low spectral resolution infrared sounders in subsidence regions.

An example comparison of RAOB and MODIS temperature and moisture is shown in Figure 18. For atmospheres with fairly monotonic, smooth temperature and moisture distribution (Figure 18), MODIS retrievals compare well to radiosondes. However, in situations with isolated layers of sharply changing temperature or moisture, MODIS is not able to capture the finer-scale structure. Improved sounding capability is expected from the Atmospheric Infrared Sounder (AIRS) on Aqua.

4.2 Continental-Scale Comparisons between MODIS and GOES TPW

On the continental-scale, MODIS TPW was compared to GOES-8 and GOES-10 sounder retrievals of TPW over the continental United States and Mexico. GOES TPW has been well validated (Schmit et al. 2002). GOES has a resolution at the sub-satellite point of 10km and uses

radiances measured from a 3 by 3 field of view area (approximately 30 km resolution) to retrieve one atmospheric profile, while MODIS has nadir resolution of 1km and uses a 5 by 5 field of view area (5 km resolution). Unlike the MODIS retrieval, GOES hourly radiance measurements are supplemented with hourly surface temperature and moisture observations as additional information in the GOES retrieval. MODIS and GOES retrieval procedures also use different first guess profiles; GOES uses a numerical model forecast, while MODIS uses the previously described regression retrieval.

Figure 19 compares MODIS TPW to TPW retrieved by the GOES-8 and GOES-10 sounders over North America for 02 June 2001 during the day and at night. The two show fairly good agreement except the MODIS TPW retrieved by regression is drier than GOES over Oklahoma, Arkansas, and the Gulf of Mexico. TPW retrieved by physical retrieval shows better agreement with GOES in these areas.

4.3 Global comparisons of MODIS products with SSMI and TOMS

Global TPW from MODIS atmospheric retrievals is compared with TPW from the Defense Meteorological Satellite Program (DMSP) Special Sensor Microwave / Imager (SSM/I) (Alishouse, 1990; Ferraro, 1996; Wentz, 1997) for 22 May 2002 in Figure 20. The SSM/I (resolution 12.5 km) retrieves products for clear or cloudy skies over ocean only, and uses the 22 and 37 GHz microwave channels. MODIS and SSM/I show similar patterns of TPW distribution and similar magnitudes, however MODIS retrievals are somewhat less moist over tropical oceans. Some of the differences can be attributed to the fact that MODIS does not retrieve cloudy pixels and, thus, does not capture the moist environment around clouds. This can affect the results even where MODIS retrievals were performed since the retrieval only requires that 5

of the 25 pixels in a 5x5 MODIS field-of-view area be clear. The remaining cloudy pixels are excluded, however the retrieval is still performed using only the clear pixels. Other differences may be attributed to the time differences between the two satellite overpasses.

MODIS total column ozone retrievals are compared with ozone from the NASA/GSFC Total Ozone Mapping Spectrometer (TOMS) (Bowman and Krueger 1985; McPeters et al. 1996, 1998) ozone measurements from the Earth Probe (EP) satellite for 22 May 2002 in Figure 21. The general distribution of ozone from TOMS is similar to that from MODIS. In order to predict the evolution of ozone on time scales of a few days to a week, reliable measurements of ozone distribution are needed. However, the TOMS instrument measures backscattered ultraviolet solar radiation and cannot provide measurements at night. High spatial resolution IR radiance measurements at 9.6 μm from MODIS allow ozone estimates during both day and night.

5. Discussion

Retrieval accuracy, computation efficiency, and retrieval validation are very important considerations when applying the operational algorithm to real time MODIS data processing. The accuracy of the retrievals depends on the actual calibration, navigation, and co-registration in the infrared band; the MOIDS is assumed to be calibrated within the instrument noise, navigated within one FOV, and co-registered within two tenths of a FOV. Several sources of errors must be addressed. First, the forward model error can introduce error in the retrievals. The forward model error may be due to the atmospheric transmittance calculation error since the transmittance is computed by a fast regression procedure rather than by an accurate line-by-line model; it may be due to inaccurate or insufficient representation of the atmospheric temperature and moisture profiles in the training data set; or it may be due to the surface uncertainties such as

surface elevation and emissivity. Improvement of the forward model is important for deriving the MODIS products with a high level of accuracy.

In addition to forward model errors, the MODIS instrument detector noise and calibration error (observation error) will have an impact on the retrieval accuracy. Large observation errors will result in poor MODIS atmospheric products. Detector to detector differences in the spectral response functions within a band have been shown to produce 0.5 to 1.0% differences in radiance measurements in the IR thermal bands (http://mcstweb.gsfc.nasa.gov/caveats/). This is seen as detector striping (called banding by some investigators) within a scene. Well-calibrated radiance measurements without (or with reduced) striping noise are expected to improve the quality of the MODIS atmospheric products presented in this paper. Cloud detection errors may also have a negative impact on the retrieval products. Regions with cloud contamination in the MODIS retrievals show elevated moisture and decreased temperature.

Computation efficiency is very important for operational MODIS data processing. Regression is a fast way to retrieve the atmospheric retrieval products, while the physical retrieval will take more computation time. It is therefore not possible to apply both the regression and physical retrieval procedures to process global MODIS data operationally at the DAAC. However, real time MODIS data received by direct broadcast MODIS stations handle a smaller amount of data and can apply both the regression and the physical retrieval processing algorithms.

One challenge is to maintain adequate global training profiles so that the statistical regression algorithm produces accurate stable atmospheric retrievals. A further challenge is to accommodate special regions such as the Sahara where the surface characteristics are unique

(very warm and dry, and the surface IR emissivity is lower than other regions). The operational MODIS algorithm is still evolving in order to meet both of these challenges.

6. Conclusions and future work

This paper describes the operational atmospheric retrieval algorithms for global and direct broadcast MODIS data processing. Because there are few time and space co-located global radiosonde observations and MODIS radiance measurements, a forward model is employed in the retrieval procedure. Some issues regarding training profiles, noise performance, forward model bias, non-unit surface emissivity over desert regions are addressed. Comparison of MODIS TPW with ground-based instrumentation at the SGP ARM-CART site revealed that MODIS agrees with the MWR with an RMS of 3.6 mm. The physical retrievals show improvements over the regression retrievals for moist cases. More comparisons with ground-based instrumentation are needed to obtain a complete assessment of the MODIS atmospheric products. Future comparisons will include other ARM-CART sites in the tropical western Pacific and in Barrow, Alaska. On large scales, MODIS products show good agreement in spatial distribution compared with GOES, SSM/I and TOMS.

Future work to improve the algorithm will include enhancing the training profile database with more radiosonde observations, particularly in polar areas that are under-represented. Surface emissivity from a global ecosystem database will be used in the training profiles to improve both the regression and physical retrievals. Improvements to the radiance bias corrections are also planned, including adding a seasonal variation to the global radiance values. The relatively high level of noise due to non-uniform detector-to-detector response (striping) will be investigated for possible reduction.

Terra MODIS algorithms have been adapted to the second MODIS instrument that was launched on the Aqua platform on 4 May 2002. The new platform will double the frequency of global coverage and allow for more consistent monitoring of temperature, moisture, and ozone. In addition, retrievals based on a combination of MODIS and AIRS radiances from Aqua will be investigated to take advantage of the high spectral resolution of AIRS and the high spatial resolution of MODIS.

Acknowledgements

The authors would like to thank the MODIS group at CIMSS for their assistance in this work including Chris Moeller, Kathy Strabala, Richard Frey, Steve Ackerman, Bryan Baum, and Hong Zhang. A special note of thanks goes to Hal Woolf who provided the MODIS fast radiative transfer model. ARM-CART site data used in this work were obtained from the Atmospheric Radiation Measurement Program sponsored by the U.S. Department of Energy, Office of Science, Office of Biological and Environmental Research, Environmental Sciences Division. SSM/I TPW data were obtained from Remote Sensing Systems. This work was funded by NASA through NAS5-31367, and NAG5-9389.

References

Ackerman, S. A., K. I. Strabala, W. P. Menzel, R. A. Frey, C. C. Moeller, and L. E. Gumley, 1998: Discriminating clear sky from clouds with MODIS. *J. Geophys. Res.*, 103, D24, 32141-32157.

Alishouse, J.C., S. Snyder, J. Vongsathorn, and R.R. Ferraro, 1990: Determination of oceanic total precipitable water from the SSM/I. IEEE Trans. Geo. Rem. Sens., 28, 811-816.

Bowman, K.P. and A.J. Krueger, 1985: A global climatology of total ozone from the Nimbus-7 Total Ozone Mapping Spectrometer", J. Geophys. Res., 90, 7967-7976.

Eyre, J.R., 1992: A bias correction scheme for simulated TOVS brightness temperatures. *ECMWF Technical Memorandum 186*. 28 pp.

____, J. R., and H. M. Woolf, 1988: Transmittance of atmospheric gases in the microwave region: a fast model. *Appl. Opt.*, **25**, 3244-3249.

Ferraro, R.R., F. Weng, N.C. Grody, and A. Basist, 1996: An eight year (1987 - 94) climatology of rainfall, clouds, water vapor, snowcover, and sea-ice derived from SSM/I measurements. Bull. of Amer. Meteor. Soc., 77, 891 - 905.

Frey, R.A., B.A. Baum, W.P. Menzel, S.A. Ackerman, C. C. Moeller, and J.D. Spinhirne, 1999: A comparison of cloud top heights computed from airborne lidar and MAS radiance data using CO_2 slicing. *J. Geophys. Res.*, 104, 24547-24555.

Hannon, S., L. L. Strow, and W. W. McMillan, 1996: Atmospheric Infrared Fast Transmittance Models: A Comparison of Two Approaches. Proceeding of SPIE conference 2830, Optical Spectroscopic Techniques and Instrumentation for Atmospheric and Space Research II.

Harris, B. A., and G. Kelly, 2001: A satellite radiance bias correction scheme for radiance assimilation. *Quart. J. Roy. Meteor. Soc.*, 127, 1453-1468.

Hayden, C. M., 1988: GOES-VAS simultaneous temperature-moisture retrieval algorithm. *J. Appl. Meteor.*, **27**, 705-733.

King, M.D., Kaufman, Y. J., Menzel, W. P. and D. Tanré, 1992: Remote sensing of cloud, aerosol, and water vapor properties from the Moderate Resolution Imaging Spectrometer (MODIS). *IEEE Trans. Geosci. Remote Sens.*, **30**, 2-27.

Li, J., 1994: Temperature and water vapor weighting functions from radiative transfer

Equation with surface emissivity and solar reflectivity. *Advances in Atmospheric Sciences*, 11, 421 - 426.

____, J., and H.-L. Huang, 1999: Retrieval of atmospheric profiles from satellite sounder measurements by use of the discrepancy principle, *Appl. Optics*, Vol. 38, No. 6, 916-923.

____, J., W. Wolf, W. P. Menzel, W. Zhang, H.-L. Huang, and T. H. Achtor, 2000: Global soundings of the atmosphere from ATOVS measurements: The algorithm and validation, *J. Appl. Meteorol.*, 39: 1248 – 1268.

____, J., C. C. Schmidt, J. P. Nelson, T. J. Schmit, and W. P. Menzel, 2001: Estimation of total ozone from GOES sounder radiances with high temporal resolution. *Journal of Atmospheric and Oceanic Technology.* 157 – 168.

McPeters, R.D, Krueger, A.J., Bhartia, P.K., Herman, J.R. et al, 1996, "Nimbus-7 Total Ozone Mapping Spectrometer (TOMS) Data Products User's Guide", NASA Reference Publication 1384, available from NASA Center for AeroSpace Information, 800 Elkridge Landing Rd, Linthicum Heights, MD 21090, USA; (301) 621-0390.

____, R.D, Krueger, A.J., Bhartia, P.K., Herman, J.R. et al, 1998, "Earth Probe Total Ozone Mapping Spectrometer (TOMS) Data Products User's Guide", NASA Reference Publication 1998-206895 , available from NASA Center for AeroSpace Information, 800 Elkridge Landing Rd, Linthicum Heights, MD 21090, USA; (301) 621-0390.

Menzel, W. P., and J. F. W. Purdom, 1994: Introducing GOES-I: The first of a new generation of geostationary operational environmental satellites. *Bull. Amer. Meteor. Soc.*, **75**, 757-781.

____, W. P., F. C. Holt, T. J. Schmit, R. M. Aune, A. J. Schreiner, G. S. Wade, and D. G. Gray, 1998. Application of the GOES-8/9 soundings to weather forecasting and nowcasting. *Bull. Amer. Meteor. Soc.*, **79**, 2059-2077.

Salisbury, J.W., and D.M. D'Aria, 1992: Emissivity of terrestrial materials in the 8-14mm atmospheric window. *Remote Sensing of the Environment*, **42**, 83-106.

Schmit, T. J., Feltz, W. F., Menzel, W. P., Jung, J., Noel, A. P., Heil, J. N., Nelson, J. P., and G.S.Wade, 2002: Validation and Use of GOES Sounder Moisture Information. *Wea. Forecasting,* **17,** 139-154.

Smith, W. L., Woolf, H. M., and W. J. Jacob, 1970: A regression method for obtaining real-time temperature and geopotential height profiles from satellite spectrometer measurements and its application to Nimbus 3 "SIRS" observations. *Mon. Wea. Rev..*, **8**, 582-603.

____, Woolf, H. M., Nieman, S. J., and T. H. Achtor, 1993: ITPP-5 - The use of AVHRR and TIGR in TOVS Data Processing. Technical Proceedings of the Seventh International TOVS Study Conference held in Igls, Austria 10 to 16 February 1993, J. R. Eyre Ed., 443-453.

Stephens, G. L., D. L. Jackson, and J. J. Bates, 1994: A comparison of SSM/I and TOVS column water vapor data over the global oceans. Meteorology and Atmospheric Physics., 54, 183-201.

Wentz F. J. 1997, "A well-calibrated ocean algorithm for SSM/I", J. Geophys. Res., Vol. 102, No. C4, pg. 8703-8718.

List of Table and Figure Captions

Table 1. MODIS Technical Specifications, from http://modis.gsfc.nasa.gov/about/specs.html.

Table 2. MODIS Band Specifications, from http://modis.gsfc.nasa.gov/about/specs.html.

Table 3. Predictors and their uncertainty used in the regression procedure

Figure 1. MODIS infrared spectral response functions (numbered by MODIS band) and nadir viewing brightness temperature spectrum of the U.S. Standard Atmosphere computed by LBL-RTM.

Figure 2. Temperature weighting functions for the MODIS IR bands 20-25, 27-36.

Figure 3. The water vapor mixing ratio weighting functions for the MODIS IR bands 20-25, 27-36.

Figure 4. The water vapor mixing ratio weighting functions for the MODIS IR bands 20-25, 27-36 for a standard atmosphere except with skin temperature 5^{o}K greater than the surface air temperature.

Figure 5. Comparison of RMS (^{o}K) for MODIS bands 24, 25, 27-29, and 31-36 for observed minus regression retrieval brightness temperatures (blue lines) with observed minus physical retrieval brightness temperatures (red lines). For reference, the instrument specification NEdT is shown in black. The top panel shows the average RMS for 43 clear-sky cases between 01 April 2001 and 01 December 2001. Each case was located at 36.6^{o} latitude and -97.5^{o} with a sensor zenith angle less than 50^{o}. The bottom panel shows the average RMS for only those cases with regression-based TPW greater than 17 mm.

Figure 6. Average (Observed-Calculated) brightness temperature for MODIS IR bands 24, 25,

27-29, and 31-36 from 63 clear sky cases at the SGP ARM-CART site from April 2001 to June 2002. Red bars indicate radiance calculations used skin temperature observed by the IRT; regression-derived skin temperature was used for the calculated radiances in the blue bars. No bias is computed for band 30 because of insufficient ozone observations for input to the forward model.

Figure 7. Comparison of skin temperature computed by MODIS regression (y-axis) with that observed by the SGP-CART IRT (x-axis) for the same cases used in Figure 6. The blue line shows a linear best fit.

Figure 8. Calculated vs. observed brightness temperatures for each MODIS IR band used in the retrieval algorithm. Each dot represents one of the 63 CART cases used in Figures 6 and 7.

Figure 9. Average monthly observed – calculated brightness temperature biases for 63 cases at the SGP ARM-CART site from April 2001 to June 2002. Biases for MODIS bands 24,25, and 27-29 are shown in the top panel and bands 31-36 in the bottom panel.

Figure 10. Histogram of actual MODIS 11μm brightness temperature observed in four granules from 2 June 2001 over the north African deserts (top), and computed from a forward model calculation using the original NOAA-88b training profiles and surface data as input (bottom).

Figure 11. Frequency of occurrence of 11mm brightness temperature in the original NOAA-88b training data set (blue) and the extended training data set including the additional desert radiosondes (red).

Figure 12. MODIS images from 20 August 2001 1729-1942UTC. Left: True color using

MODIS reflectance from bands 1, 4, 3 as red, green, and blue, respectively; Right: MODIS band 31 radiance. Images obtained from University of Wisconsin-Madison's direct broadcast (http://eosdb.ssec.wisc.edu/modisdirect/).

Figure 13. Total precipitable water (mm) from August 20, 2001 retrieved from GOES-8 (left), new operational MODIS (center), and MODIS without the 11mm brightness temperature zones (right). The MODIS granule began at 1735 UTC and GOES at 1800 UTC.

Figure 14. 11μm brightness temperature broken down into the same seven zones used in the retrieval algorithm for the same case as in Figure 13. The areas that show the most improvement in the comparison in Figure 13 are in the warmest two brightness temperature classes.

Figure 15. Emissivity spectral measurements (%) from data obtained through the NASA Jet Propulsion Lab's spectral library (http://speclib.jpl.nasa.gov) for two silicates commonly found in desert regions, cyclosilicates (black line) and tectosilicates (red line).

Figure 16: Brightness temperature increment (^{o}K) for bands 24 and 25 individually (dash-dot and dash, respectively) and for the difference between bands25-24 (solid line). Calculations used a standard U.S. mid-latitude summer atmosphere.

Figure 17. Comparison of TPW from MODIS regression (red dot), GOES-8 (blue diamonds), and radiosonde (black cross) with the SGP ARM-CART microwave radiometer (MWR) in millimeters. 64 cases from April 2001 to June 2002 are shown in the comparison. The dotted line shows a one-to-one correspondence.

Figure 18. Comparison of temperature (left, ^{o}K) and mixing ratio (right, g/kg) on 01 August 2001 from the average of 9 MODIS profiles in a 3x3 retrieval area surrounding the SGP ARM-CART site at 1705 UTC (blue), and a radiosonde launched at 1728 UTC (black).

In this situation where the temperature and moisture profiles are smooth, MODIS captures the vertical structure fairly well.

Figure 19. Total precipitable water (mm) for 02 June 2001 over North America retrieved by MODIS regression (left), MODIS physical (center), and GOES-8 and GOES-10 (combined, right). The top column shows daytime retrievals (4 MODIS granules from 1640, 1645, 1820, 1825 UTC; GOES at 1800UTC), and the bottom column nighttime (MODIS 0435, 0440, 0445, 0615, 0620 UTC; GOES 06 UTC). The slight discontinuity visible in Oklahoma in the MODIS daytime retrievals occurs where granules from the two subsequent overpasses, separated by 1 hour and 40 minutes, intersect.

Figure 20. MODIS TPW (mm, upper panel) and SSM/I f-14 TPW (mm, lower panel) distribution on 22 May 2002. Retrievals from ascending and descending passes were averaged to obtain these values. The color scale is the same for both MODIS and SSM/I and is shown below the two images. SSM/I data were obtained through http://www.ssmi.com. MODIS data was degraded to 25 km resolution from the original 5 km resolution for this figure.

Figure 21. Total column ozone (Dobson units) for 22 May 2002 for MODIS (top) and TOMS (bottom). TOMS data was obtained from http://toms.gsfc.nasa.gov/ozone/ozone.html.

Table 1: MODIS Technical Specifications, from http://modis.gsfc.nasa.gov/about/specs.html.

Orbit:	705 km altitude, sun-synchronous, 10:30 a.m. descending node
Scan Rate:	20.3 rpm, cross track
Swath Dimensions:	2330 km (cross track) by 10 km (along track at nadir)
Quantization:	12 bits
Spatial Resolution:	250 m (bands 1-2), 500 m (bands 3-7), 1000 m (bands 8-36)

Table 2: MODIS Band Specifications, from http://modis.gsfc.nasa.gov/about/specs.html.

Primary use	Band	Bandwith[1]	Spectral radiance[2]	Required SNR[3]
Land/Cloud/Aerosols Boundaries	1	620-670	21.8	128
	2	841-876	24.7	201
Land/Cloud/Aerosols Properties	3	459-479	35.3	243
	4	545-565	29.0	228
	5	1230-1250	5.4	74
	6	1628-1652	7.3	275
	7	2105-2155	1.0	110
Ocean Color/ Phytoplankton /Biogeochemistry	8	405-420	44.9	880
	9	438-448	41.9	838
	10	483-493	32.1	802
	11	526-536	27.9	754
	12	546-556	21.0	750
	13	662-672	9.5	910
	14	673-683	8.7	1087
	15	743-753	10.2	586
	16	862-877	6.2	516
Atmospheric Water Vapor	17	890-920	10.0	167
	18	931-941	3.6	57
	19	915-965	15.0	250
Primary use	Band	Bandwith[1]	Spectral radiance[2]	Required NEΔT[4] (K)
Surface Temperature	20	3.660-3.840	0.45 (300K)	0.05
	21	3.929-3.989	2.38 (335K)	2.00
	22	3.929-3.989	0.67 (300K)	0.07
	23	4.020-4.080	0.79 (300K)	0.07
Temperature profile	24	4.433-4.498	0.17 (250K)	0.25
	25	4.482-4.549	0.59 (275K)	0.25
Cirrus Clouds/water vapor	26	1.360-1.390	6.00	150 (SNR)
	27	6.535-6.895	1.16 (240K)	0.25
	28	7.175-7.475	2.18 (250K)	0.25
	29	8.400-8.700	9.58 (300K)	0.05
Ozone	30	9.580-9.880	3.69 (250K)	0.25

Primary use	Band	Bandwith[1]	Spectral radiance[2]	Required SNR[3]
Surface Temperature	31	10.780-11.280	9.55 (300K)	0.05
	32	11.770-12.270	8.94 (300K)	0.05
Temperature profile	33	13.185-13.485	4.52 (260K)	0.25
	34	13.485-13.785	3.76 (250K)	0.25
	35	13.785-14.085	3.11 (240K)	0.25
	36	14.085-14.385	2.08 (220K)	0.35

[1] Bands 1 to 19 are in nm, and bands 20 to 36 are in μm; [2] Spectral Radiance values are (W m^{-2} sr^{-1} μm^{-1}); [3] SNR = Signal-to-noise ratio; [4] NEΔT = Noise-equivalent temperature difference

Table 3: Predictors and their uncertainty used in the regression procedure

Predictor	Noise used in MOD07 algorithm	Post-launch NEdT averaged over detectors
Band 25-24 BT (4.47 – 4.52μm)	0.75 ^{o}K	0.163 ^{o}K (band 24) 0.086 ^{o}K (band 25)
Band 27 BT (6.7μm)	0.75^{o}K	0.376 ^{o}K
Band 28 BT (7.3μm)	0.75^{o}K	0.193 ^{o}K
Band 29 BT (8.55μm)	0.189^{o}K	0.189 ^{o}K
Band 30 BT (9.73μm)	0.75^{o}K	0.241 ^{o}K
Band 31 BT (11μm)	0.167^{o}K	0.167 ^{o}K
Band 32 BT (12μm)	0.192^{o}K	0.192 ^{o}K
Band 33 BT (13.3μm)	0.75^{o}K	0.308 ^{o}K
Band 34 BT (13.6μm)	0.75^{o}K	0.379 ^{o}K
Band 35 BT (13.9μm)	0.75^{o}K	0.366 ^{o}K
Band 36 BT (14.2μm)	1.05^{o}K	0.586 ^{o}K
Surface Pressure	5 hPa	--
Latitude	0.001^{o}	--

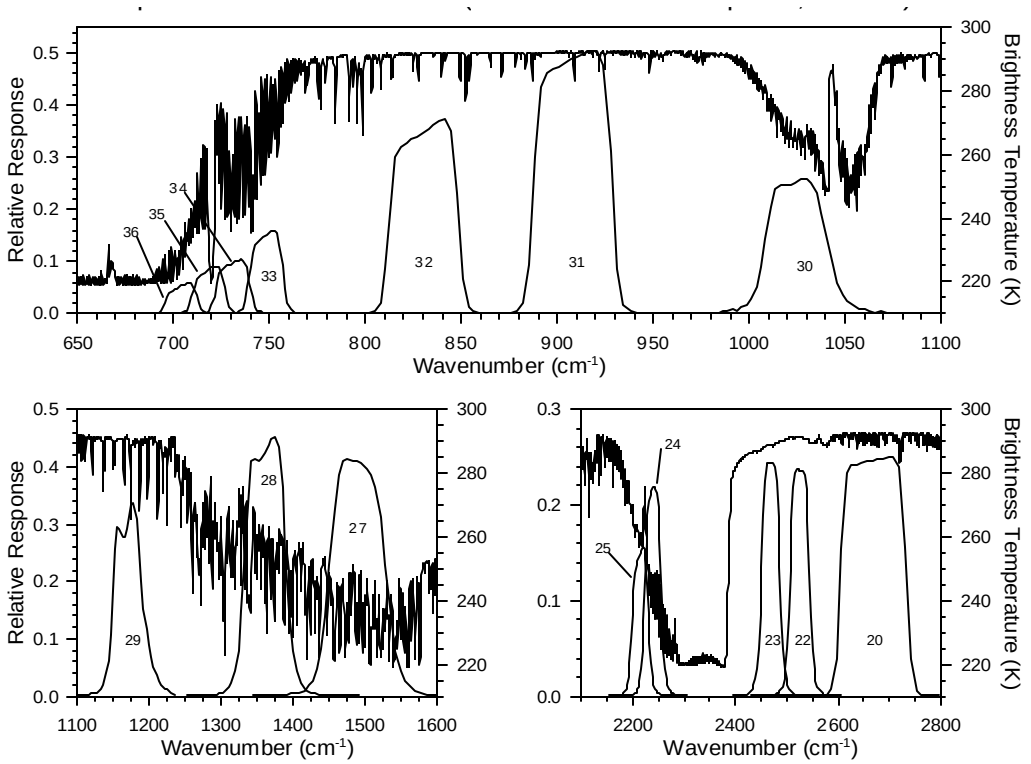

Figure 1: MODIS infrared spectral response functions (numbered by MODIS band) and nadir viewing brightness temperature spectrum of the U.S. Standard Atmosphere computed by LBL-RTM.

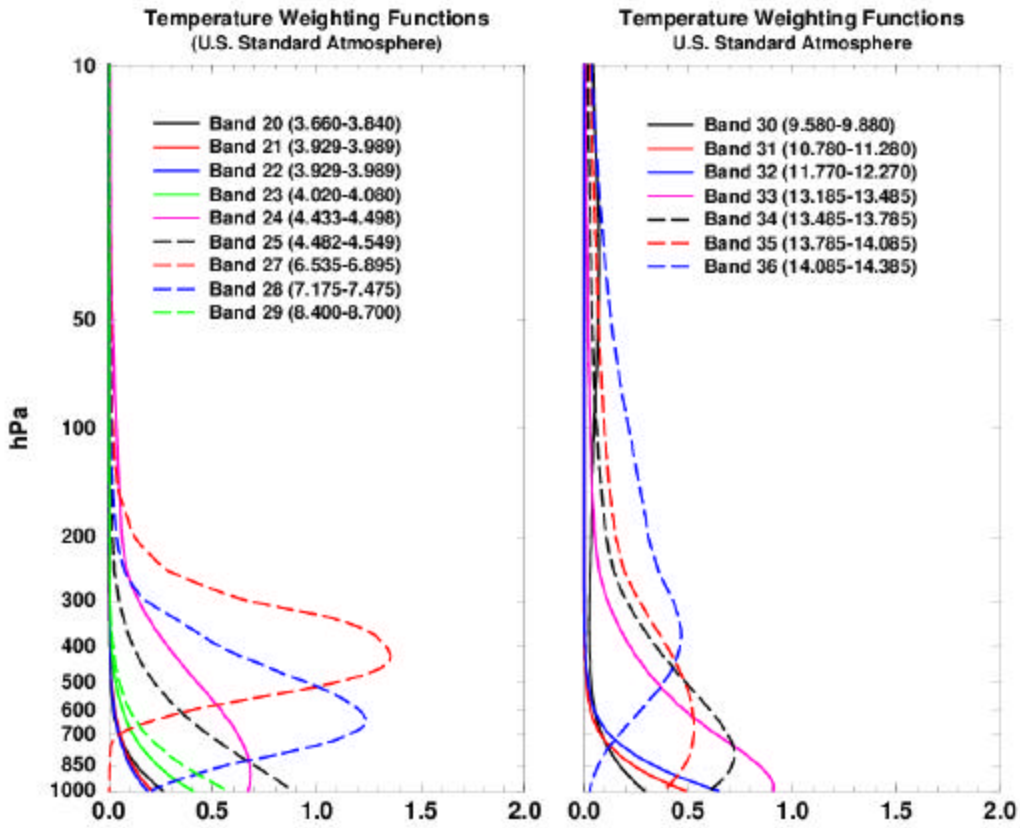

Figure 2: Temperature weighting functions for the MODIS IR bands 20-25, 27-36.

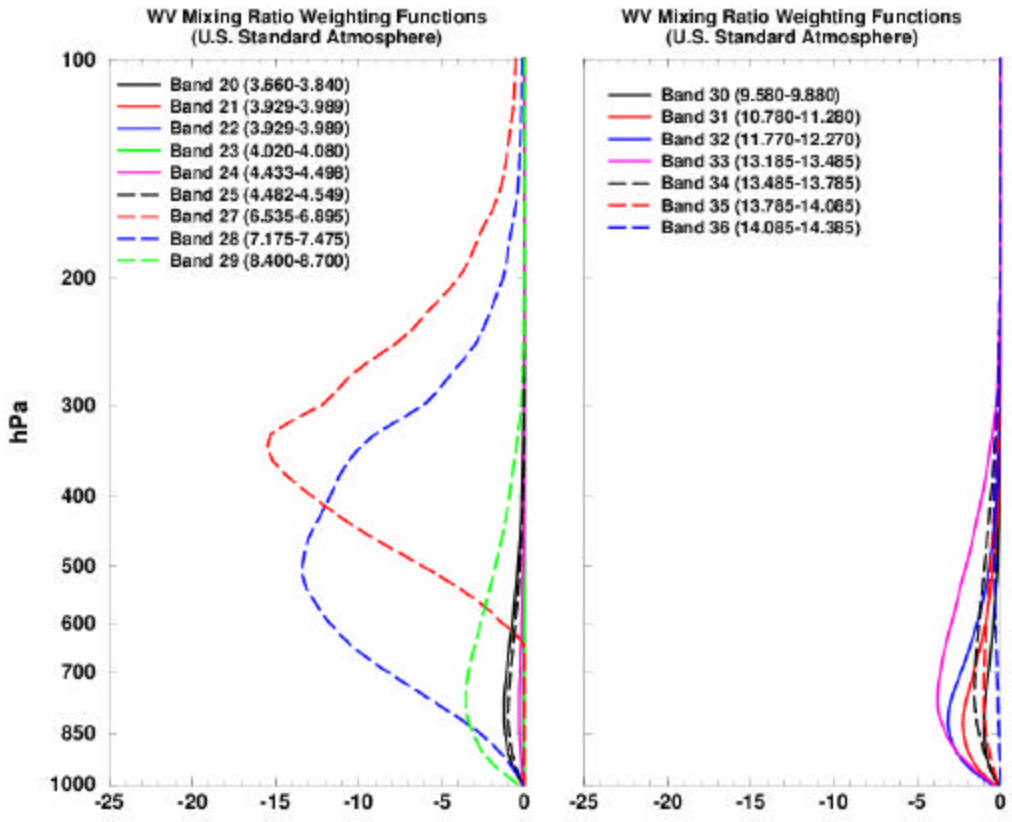

Figure 3: The water vapor mixing ratio weighting functions for the MODIS IR bands 20-25, 27-36.

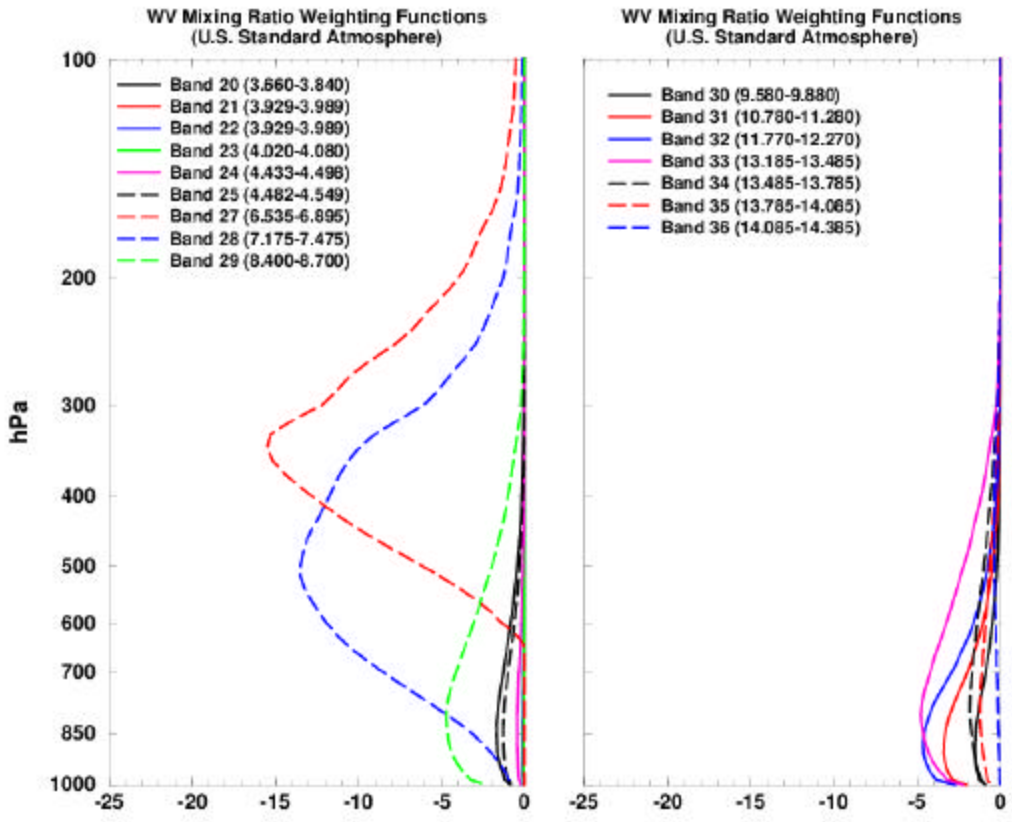

Figure 4: The water vapor mixing ratio weighting functions for the MODIS IR bands 20-25, 27-36 for a standard atmosphere except with skin temperature 5^{o}K greater than the surface air temperature.

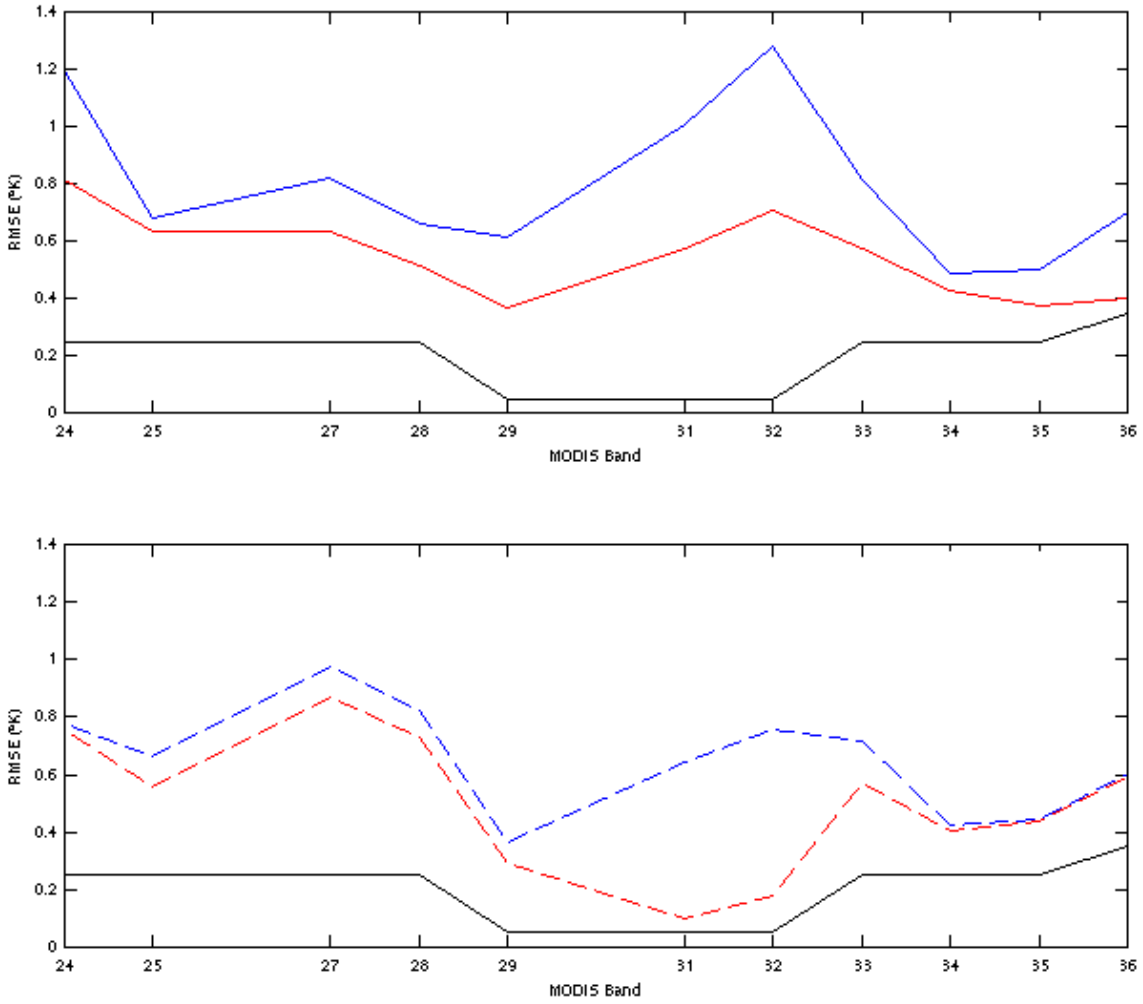

Figure 5. Comparison of RMS (^{o}K) for MODIS bands 24, 25, 27-29, and 31-36 for observed minus regression retrieval brightness temperatures (blue lines) with observed minus physical retrieval brightness temperatures (red lines). For reference, the instrument specification NEdT is shown in black. The top panel shows the average RMS for 43 clear-sky cases between 01 April 2001 and 01 December 2001. Each case was located at 36.6^{o} latitude and –97.5^{o} with a sensor zenith angle less than 50^{o}. The bottom panel shows the average RMS for only those cases with regression-based TPW greater than 17 mm.

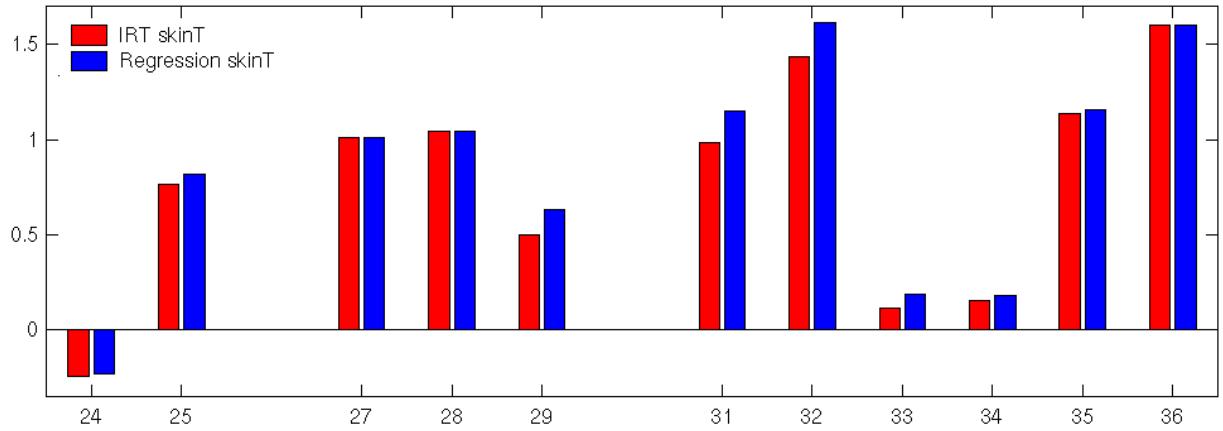

Figure 6: Average (Observed-Calculated) brightness temperature for MODIS IR bands 24, 25, 27-29, and 31-36 from 63 clear sky cases at the SGP ARM-CART site from April 2001 to June 2002. Red bars indicate radiance calculations used skin temperature observed by the IRT; regression-derived skin temperature was used for the calculated radiances in the blue bars. No bias is computed for band 30 because of insufficient ozone observations for input to the forward model.

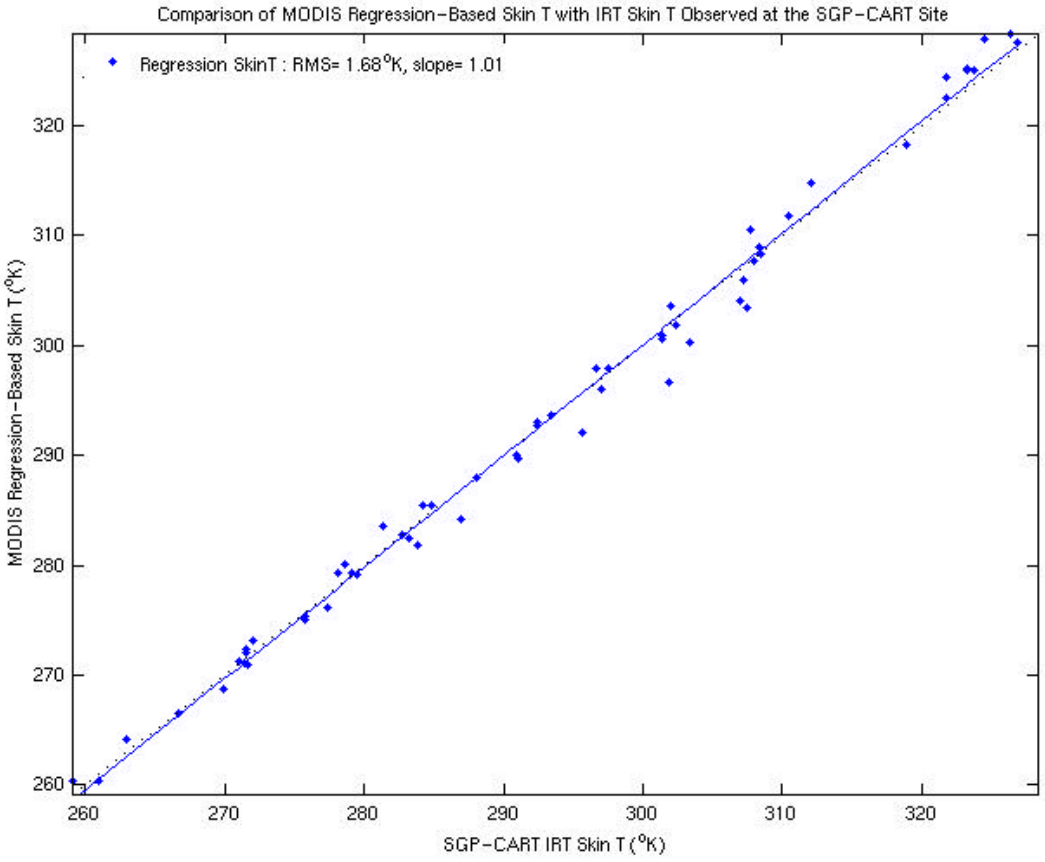

Figure 7: Comparison of skin temperature computed by MODIS regression (y-axis) with that observed by the SGP-CART IRT (x-axis) for the same cases used in Figure 6. The blue line shows a linear best fit.

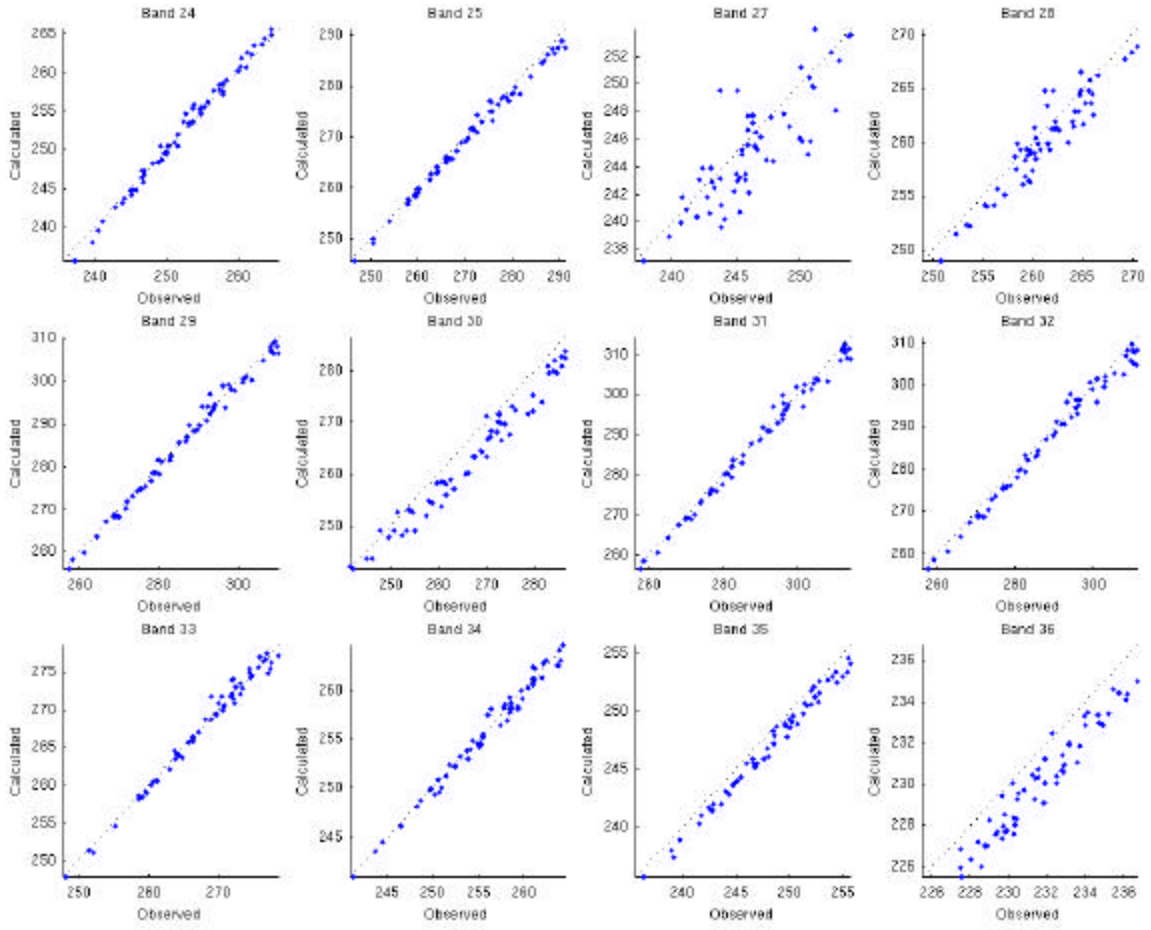

Figure 8: Calculated vs. observed brightness temperatures for each MODIS IR band used in the retrieval algorithm. Each dot represents one of the 63 CART cases used in Figures 6 and 7.

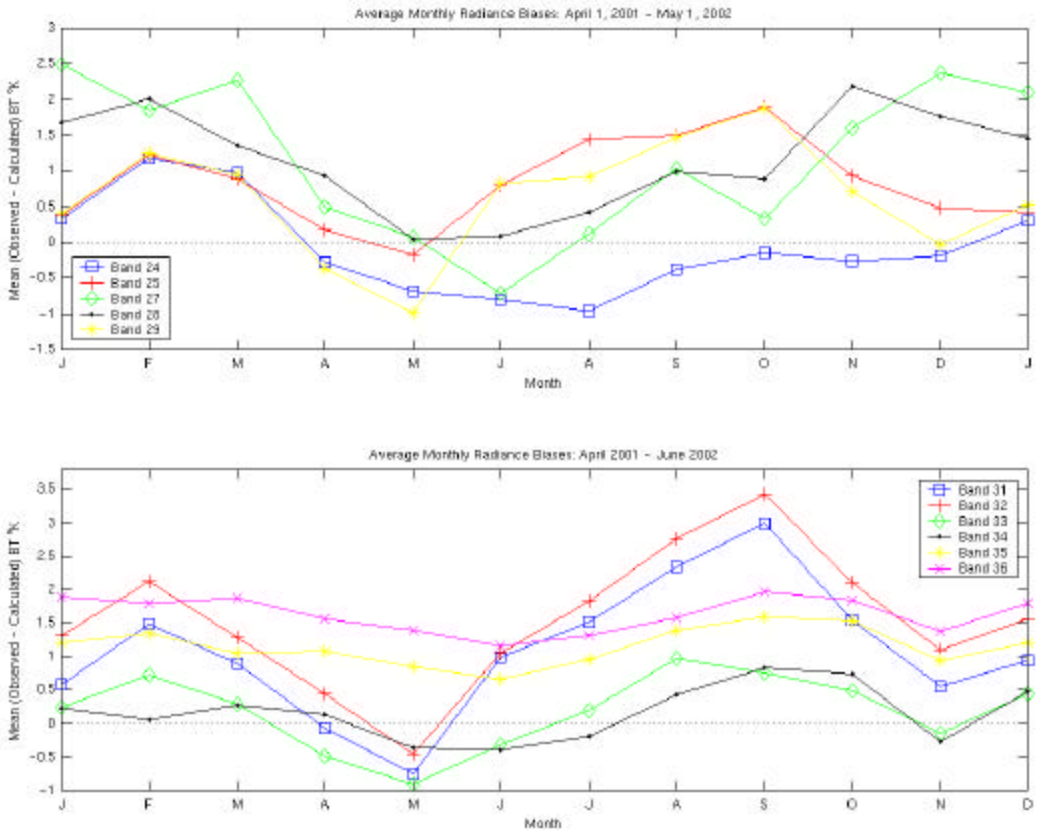

Figure 9: Average monthly observed – calculated brightness temperature biases for 63 cases at the SGP ARM-CART site from April 2001 to June 2002. Biases for MODIS bands 24,25, and 27-29 are shown in the top panel and bands 31-36 in the bottom panel.

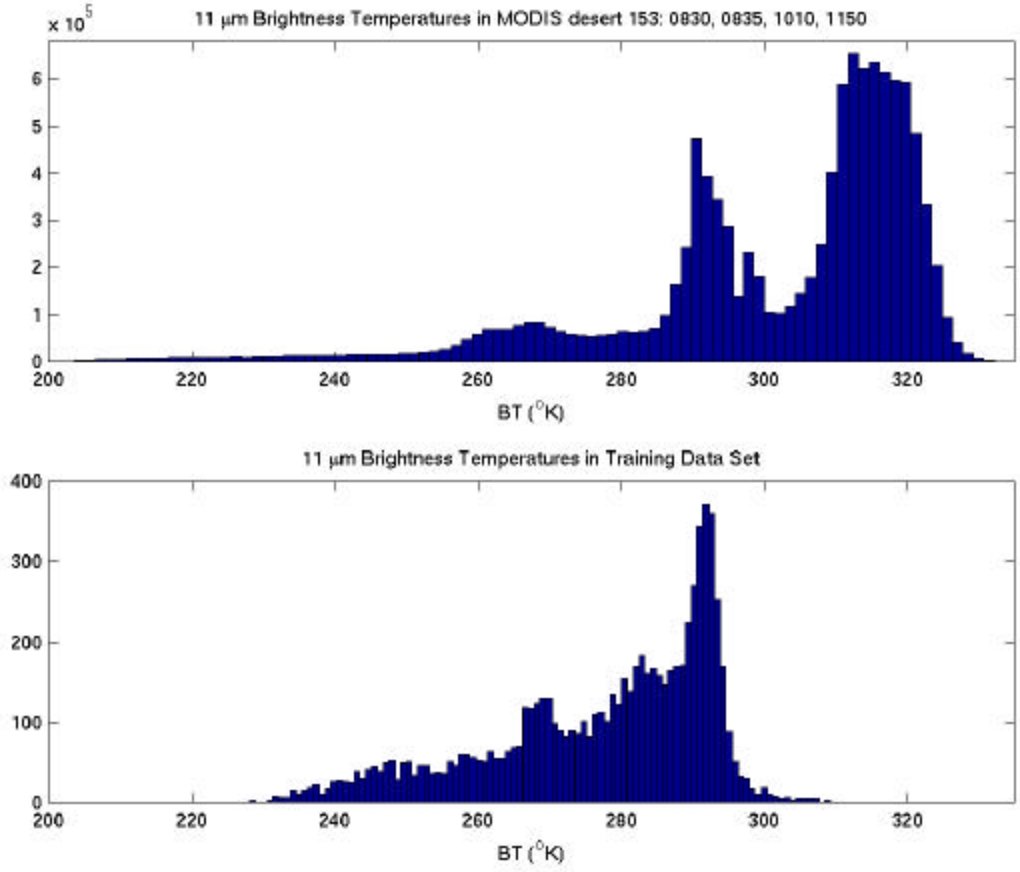

Figure 10. Histogram of actual MODIS 11μm brightness temperature observed in four granules from 02 June 2001 over the north African deserts (top), and computed from a forward model calculation using the original NOAA-88b training profiles and surface data as input (bottom).

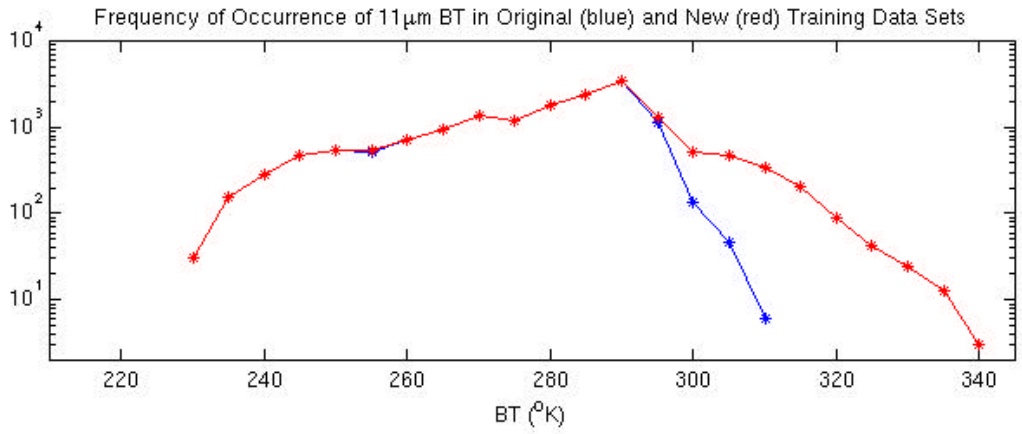

Figure 11. Frequency of occurrence of 11mm brightness temperature in the original NOAA-88b training data set (blue) and the extended training data set including the additional desert radiosondes (red).

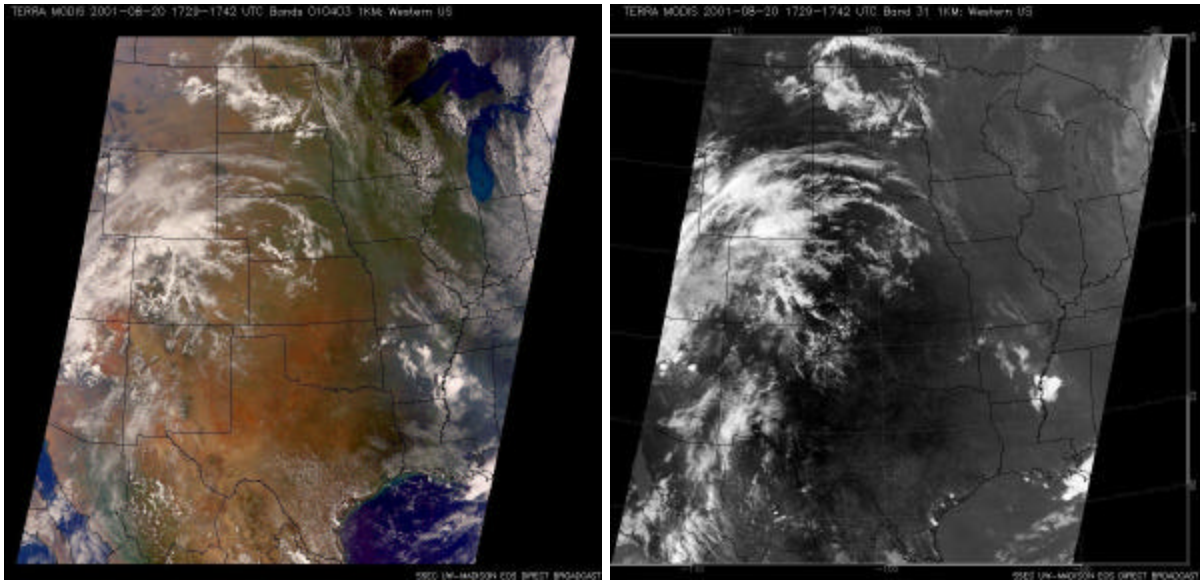

Figure 12. MODIS images from 20 August 2001 1729-1942UTC. Left: True color using MODIS reflectance from bands 1, 4, 3 as red, green, and blue, respectively; Right: MODIS band 31 radiance. Images obtained from University of Wisconsin-Madison's direct broadcast (http://eosdb.ssec.wisc.edu/modisdirect/).

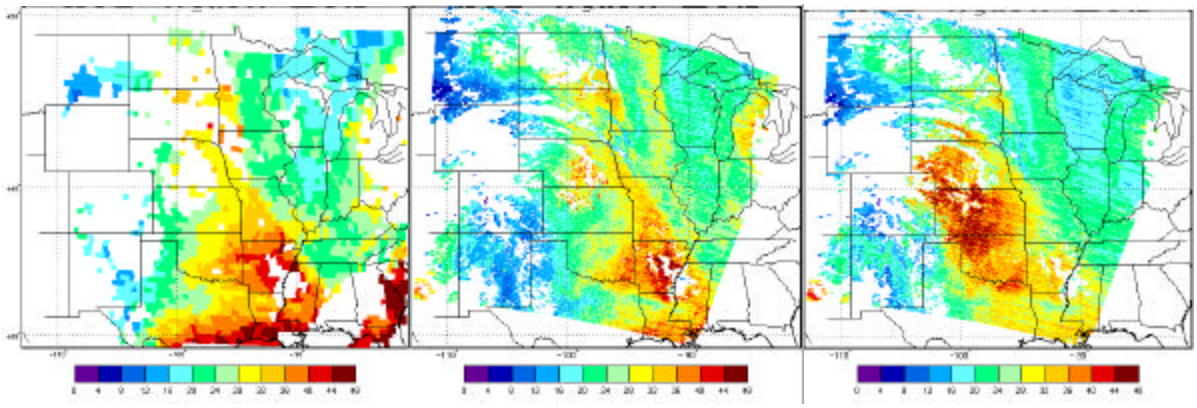

Figure 13. Total precipitable water (mm) from 20 August 2001 retrieved from GOES-8 (left), new operational MODIS (center), and MODIS without the 11mm brightness temperature zones (right). The MODIS granule began at 1735 UTC and GOES at 1800 UTC.

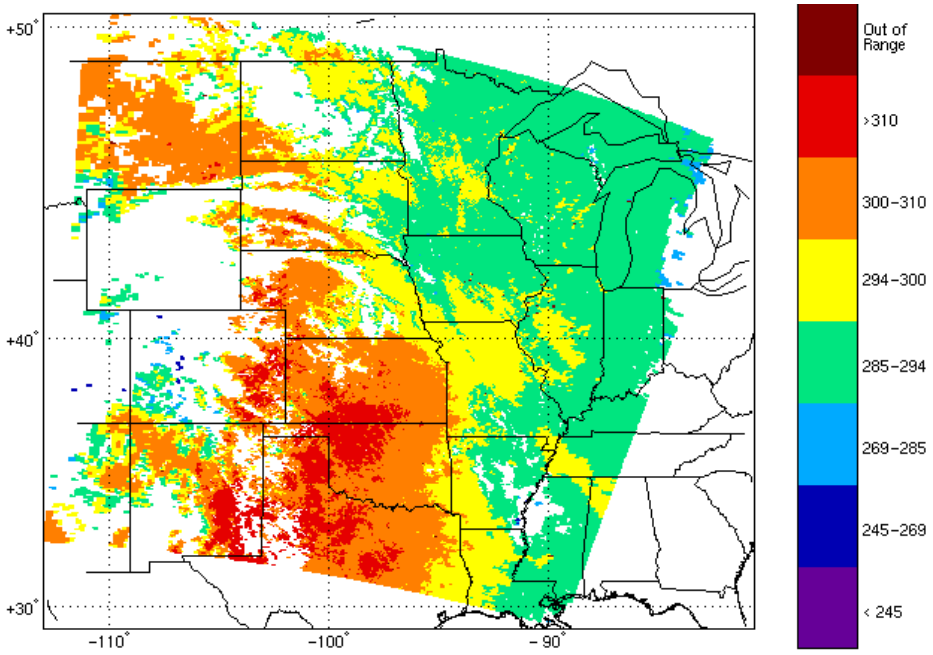

Figure 14. 11μm brightness temperature broken down into the same seven zones used in the retrieval algorithm for the same case as in Figure 13. The areas that show the most improvement in the comparison in Figure 13 are in the warmest two brightness temperature classes.

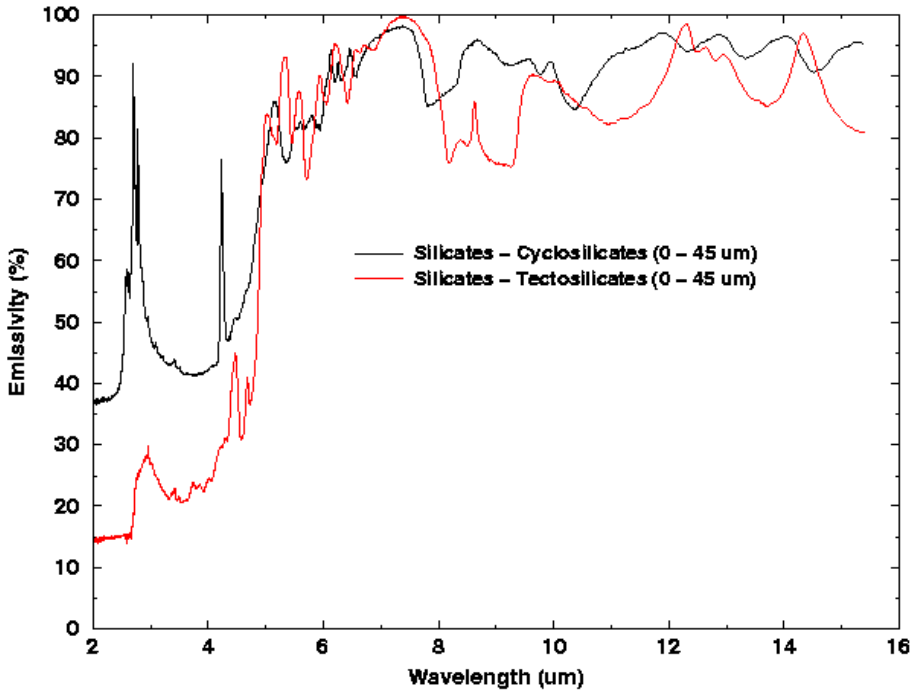

Figure 15: Emissivity spectral measurements (%) from data obtained through the NASA Jet Propulsion Lab's spectral library (http://speclib.jpl.nasa.gov) for two silicates commonly found in desert regions, cyclosilicates (black line) and tectosilicates (red line).

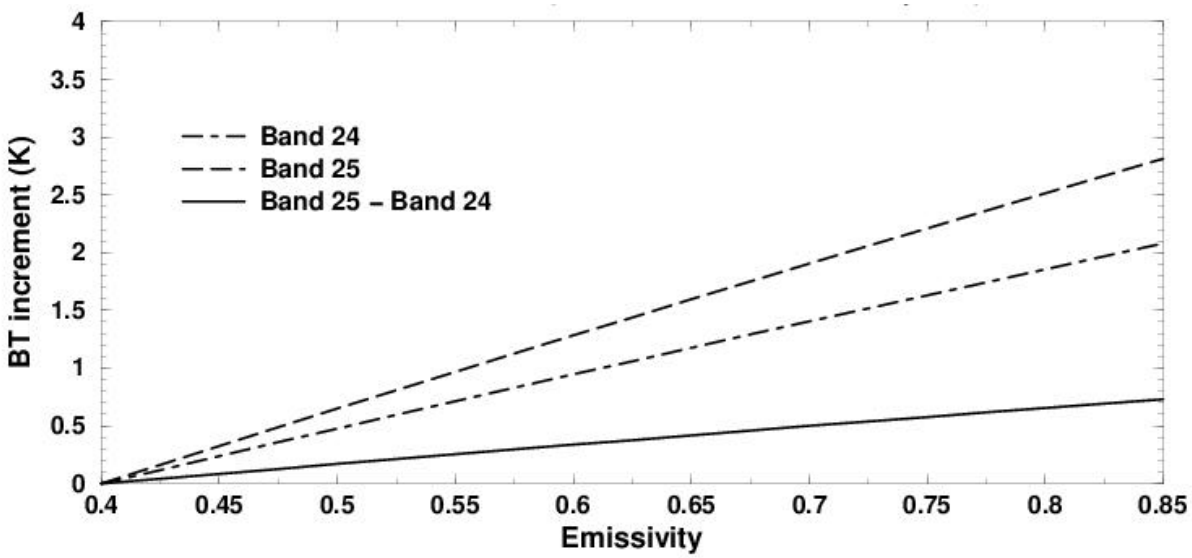

Figure 16: Brightness temperature increment (^{o}K) for bands 24 and 25 individually (dash-dot and dash, respectively) and for the difference between bands 25-24 (solid line). Calculations used a standard U.S. mid-latitude summer atmosphere.

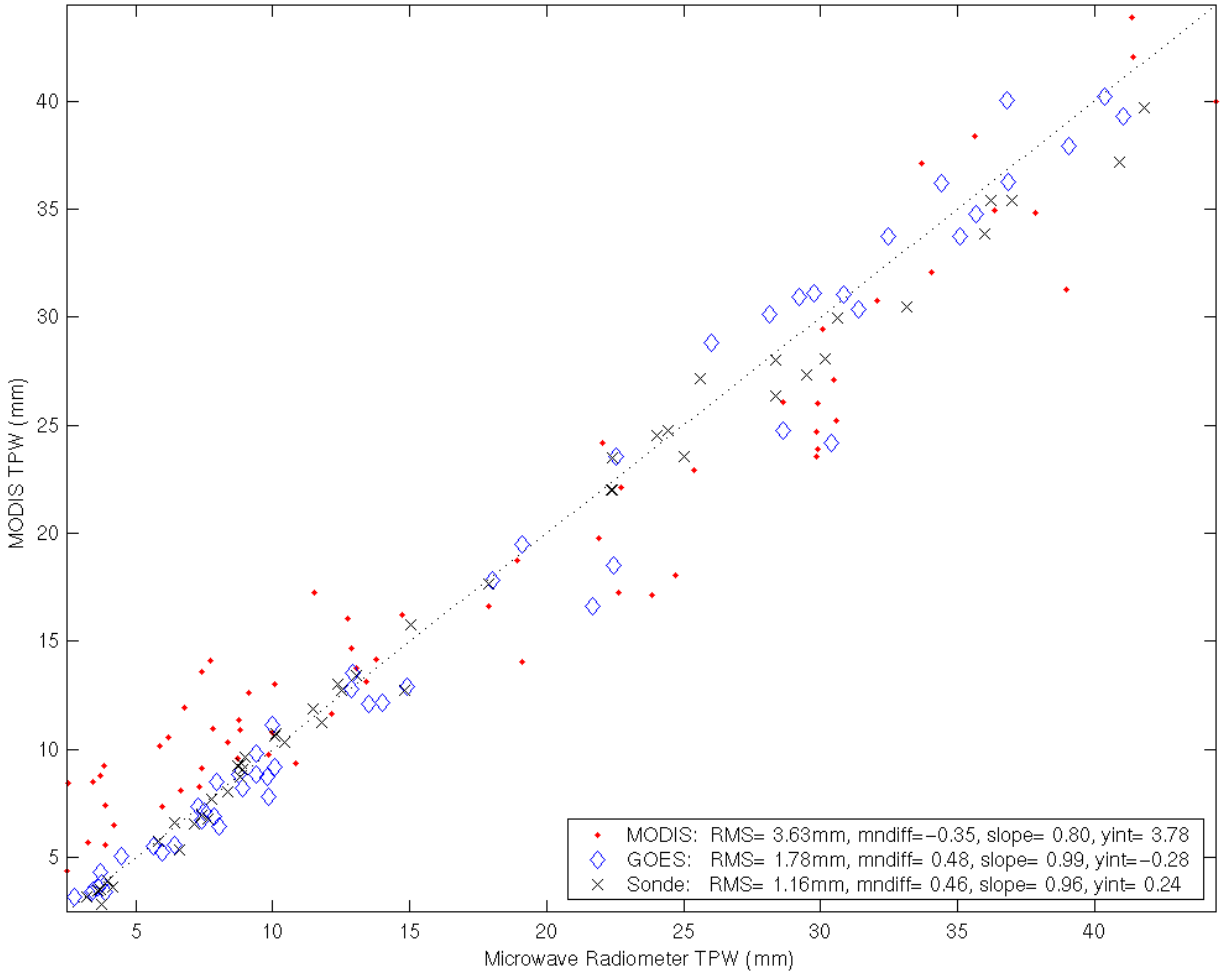

Figure 17. Comparison of TPW from MODIS regression (red dot), GOES-8 (blue diamonds), and radiosonde (black cross) with the SGP ARM-CART microwave radiometer (MWR) in millimeters. 64 cases from April 2001 to June 2002 are shown in the comparison. The dotted line shows a one-to-one correspondence.

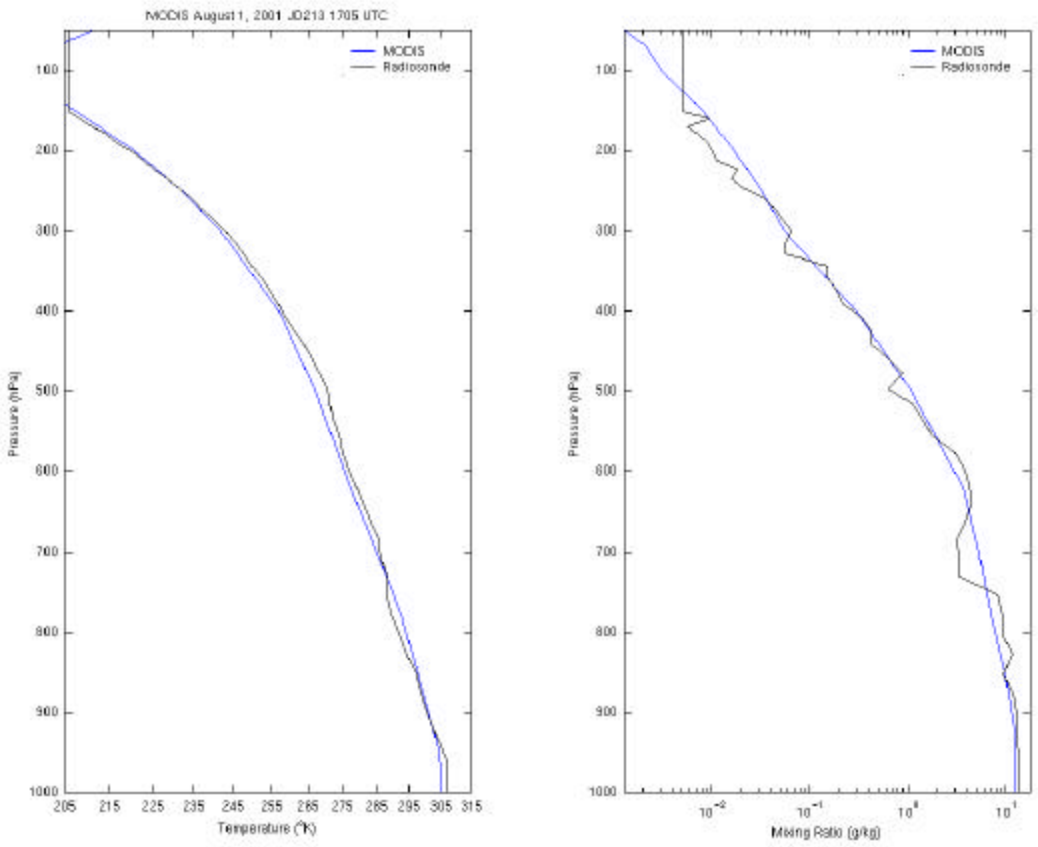

Figure 18. Comparison of temperature (left, ^{o}K) and mixing ratio (right, g/kg) on 01 August 2001 from the average of 9 MODIS profiles in a 3x3 retrieval area surrounding the SGP ARM-CART site at 1705 UTC (blue), and a radiosonde launched at 1728 UTC (black). In this situation where the temperature and moisture profiles are smooth, MODIS captures the vertical structure fairly well.

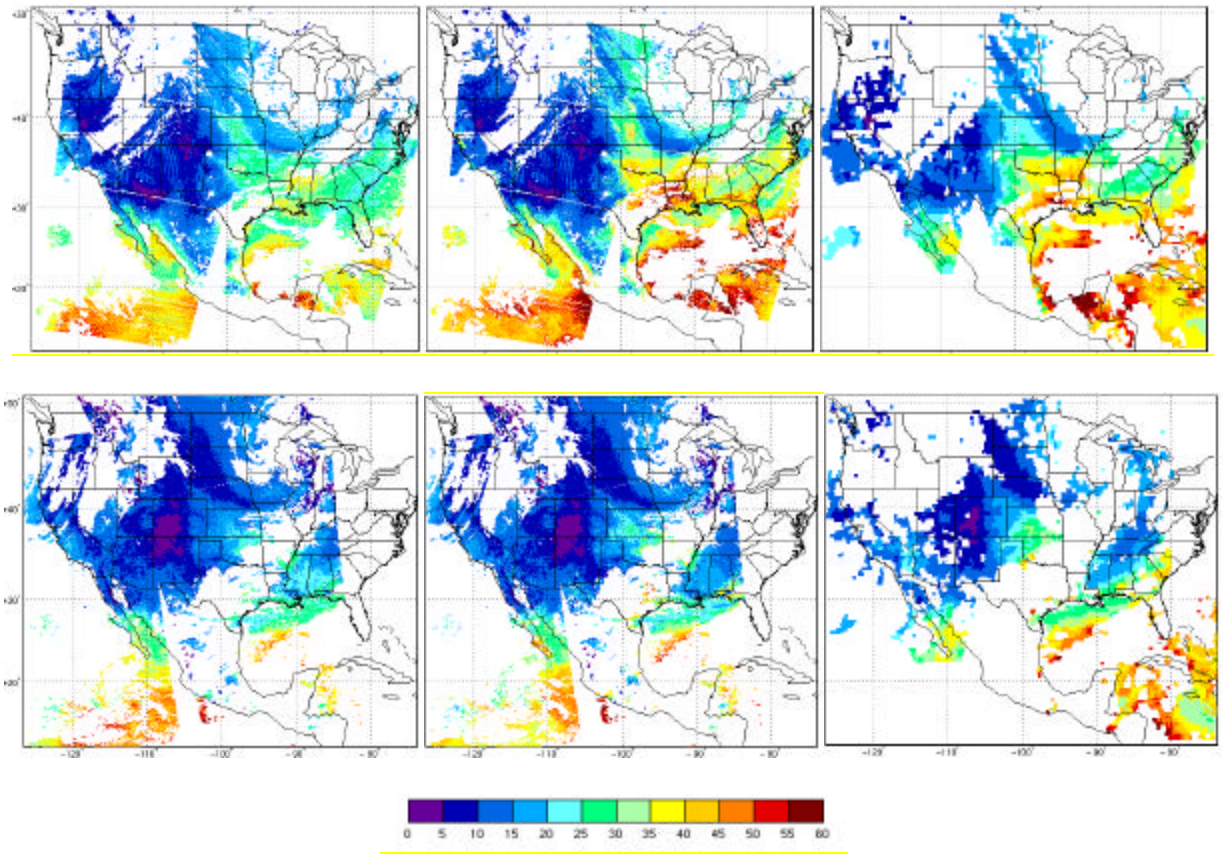

Figure 19. Total precipitable water (mm) for 02 June 2001 over North America retrieved by MODIS regression (left), MODIS physical (center), and GOES-8 and GOES-10 (combined, right). The top column shows daytime retrievals (4 MODIS granules from 1640, 1645, 1820, 1825 UTC; GOES at 1800UTC), and the bottom column nighttime (MODIS 0435, 0440, 0445, 0615, 0620 UTC; GOES 06 UTC). The slight discontinuity visible in Oklahoma in the MODIS daytime retrievals occurs where granules from the two subsequent overpasses, separated by 1 hour and 40 minutes, intersect.

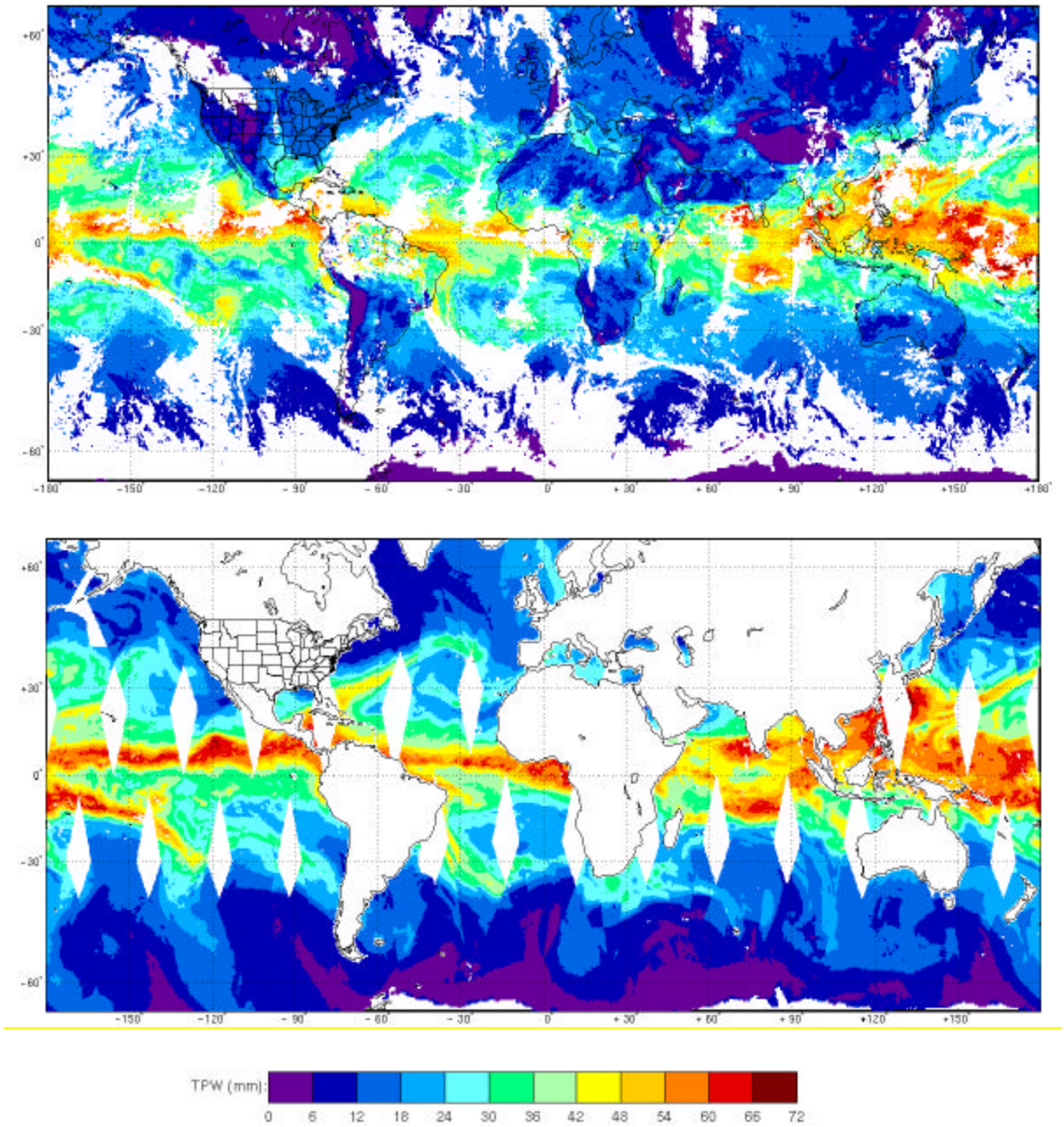

Figure 20. MODIS TPW (mm, upper panel) and SSM/I f-14 TPW (mm, lower panel) distribution on 22 May 2002. Retrievals from ascending and descending passes were averaged to obtain these values. The color scale is the same for both MODIS and SSM/I and is shown below the two images. SSM/I data were obtained through http://www.ssmi.com. MODIS data was degraded to 25 km resolution from the original 5 km resolution for this figure.

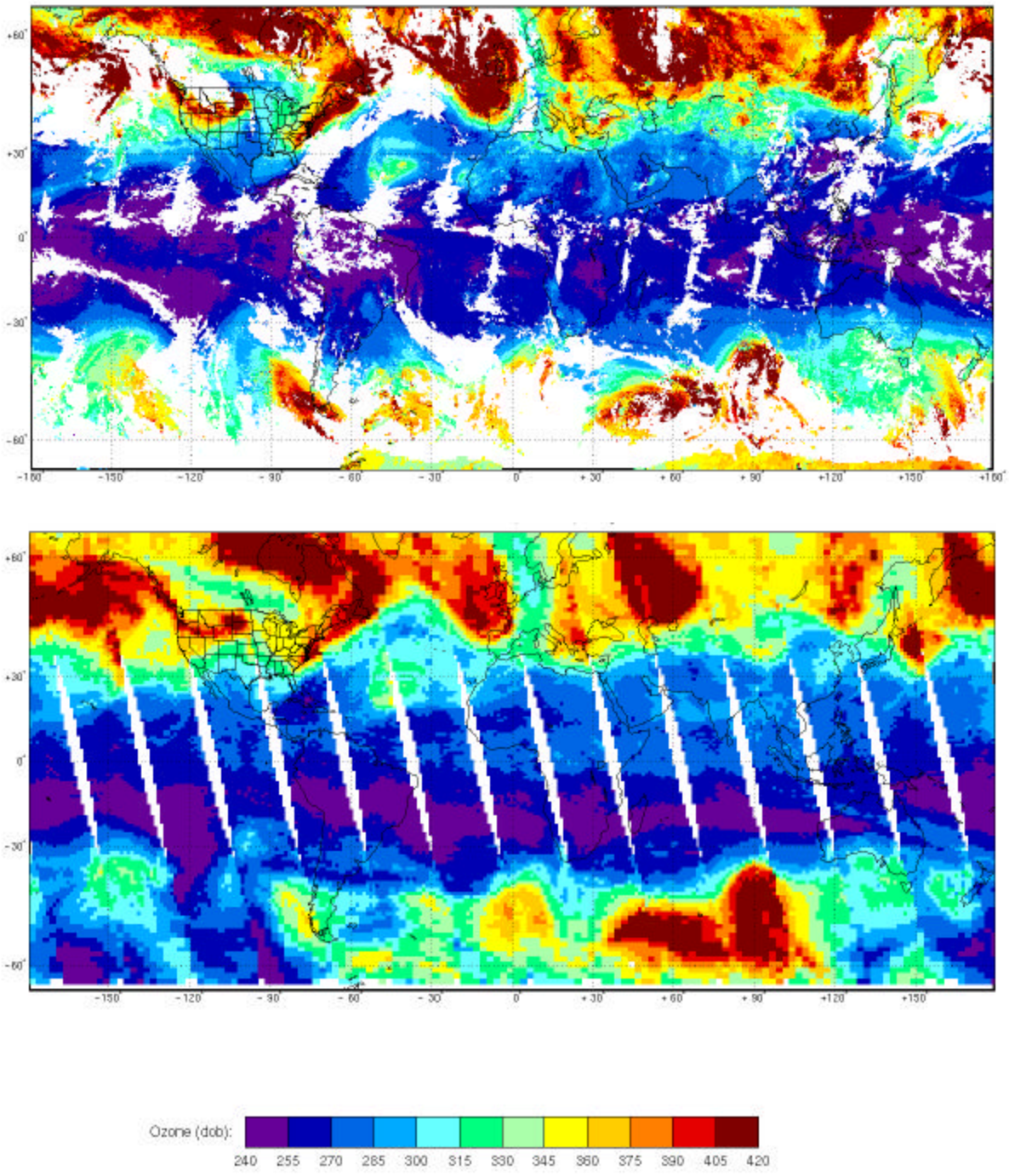

Figure 21. Total column ozone (Dobson units) for 22 May 2002 for MODIS (top) and TOMS (bottom). TOMS data was obtained from http://toms.gsfc.nasa.gov/ozone/ozone.html.